Random antiferromagnetic quantum spin chains

Daniel S. Fisher
Physics Department, Harvard University, Cambridge, Massachusetts 02138
(Received 17 March 1994)

The properties of spin-$\frac{1}{2}$ antiferromagnetic chains with various types of random exchange coupling are studied via an asymptotically exact decimation renormalization-group transformation, which is a generalization of that introduced by Dasgupta and Ma. Random-singlet phases occur in which each spin is paired with one other spin that may be very far away; more exotic phases also occur. The behavior of typical and mean correlation functions is analyzed and found to be very different, with very small sets of spins dominating the latter at long distances as well as the low-temperature thermodynamics. Some of the phase transitions that occur between antiferromagnetically ordered phases and random singlet or other antiferromagnetic phases are also analyzed. For example, if a small uniaxial anisotropy perturbation is added to a random Heisenberg antiferromagnetic chain, a transition occurs from a random-singlet phase to an Ising antiferromagnetic phase, as the anisotropy changes sign from easy plane to easy axis. The staggered magnetization vanishes at the transition with critical exponent $\beta=8/(1+\sqrt{7})$. Possible implications for the properties of random quantum magnetic systems in higher dimensions are briefly discussed.

I. INTRODUCTION

Quantum spin chains exhibit a wide variety of interesting phenomena at low temperatures that are controlled by the behavior of their ground states and low-lying excitations. Broken symmetry, quasi-long-range order, effects of topology of the rotation group and assorted types of phase transitions are all found at zero temperature and have been analyzed via exact solutions, particularly Bethe's ansatz, mapping onto other solvable problems, renormalization-group treatments of effective long-wavelength actions, conformal covariance, exact numerical diagonalizations, quantum Monte Carlo simulations, series expansions, and by numerical renormalization-group computations.[1]

In the presence of quenched randomness, far less is known. In some regimes, the randomness is irrelevant at low energies and can be treated perturbatively.[2] However, for quantum spin chains that can be mapped to free fermion systems (i.e., XY spin chains and transverse field Ising chains), localization of the wave functions of the fermions suggests some kind of localization of spin excitations, although even in these cases the understanding of the low-energy behavior is far from complete.[3–6] For more complicated situations such as random Heisenberg chains and systems with phase transitions as functions of anisotropy, even less is known. The competition between localization effects and order can certainly play a role, and because of the time independence of the randomness, the effects of rare regions on macroscopic properties will be far more important than for classical systems with quenched disorder. Fortunately, the one-dimensional nature of quantum spin chains enables, even in the presence of quenched randomness, progress to be made by real-space renormalization-group methods.[7] As we shall see, these can be used, somewhat surprisingly, to obtain new *exact* results for the long-length scale, low-frequency behavior of randomness-dominated phases as well as the critical behavior near to various zero-temperature phase transitions that occur. The basic method follows a novel approach originated by Dasgupta and Ma,[8] and Ma, Dasgupta, and Hu.[9]

Dasgupta and Ma[8] studied the properties of antiferromagnetic Heisenberg spin-$\frac{1}{2}$ chains with random exchange couplings. They analyzed the low-energy behavior via an approximate renormalization-group transformation in which the strongest exchange is decimated away, yielding a new effective exchange coupling between what were third-nearest neighbors. The procedure is iterated and the distribution of renormalized exchange couplings kept track of. This distribution becomes extremely broad,[8] which makes the approximation better and better. It is this crucial feature of the renormalization-group (RG) transformation which will enable us to obtain many new exact results for this and other random quantum spin chains. Although Dasgupta and Ma[8] did not find exact fixed points of their transformation, they guessed essentially the correct behavior from numerical studies and an approximate analysis of the RG flow equation for the distribution of exchange couplings, finding a zero-temperature phase which has since been dubbed a "random-singlet" phase.[10]

In a recent paper,[11] the present author used a generalization of Dasgupta and Ma's method to analyze the critical behavior of random transverse field Ising spin chains, which are related to two-dimensional (2D) Ising models with couplings that are uniform along strips, but random from strip to strip—the partially-exactly-solvable McCoy-Wu model.[5,6] In this paper we will extend Dasgupta and Ma's results on Heisenberg antiferromagnetic chains to analyze more general antiferromagnetic spin chains including the effects of anisotropy, the phase diagrams, the nature of disordered phases, and some of the phase transitions that can occur, in particular, that from a localized random singlet phase to an Ising antiferromagnet as a function of anisotropy.

A. Model and phase diagrams

The primary systems that we will consider are random antiferromagnetic XYZ spin-$\frac{1}{2}$ chains with nearest-neighbor couplings with the Hamiltonian

$$\mathcal{H}=\sum_n [J_n^x S_n^x S_{n+1}^x + J_n^y S_n^y S_{n+1}^y + J_n^z S_n^z S_{n+1}^z] \ . \tag{1.1}$$

We will focus in particular on the simpler XY spin chain for which all the $\{J_n^z\}$ are zero and the XXZ chain with $J_n^x = J_n^y \equiv J_n^\perp$ for which the total $S_T^z \equiv \sum_n S_n^z$ is conserved. By rotating the spin variables on alternate sites, one can choose all the $\{J_n^x\}$ and $\{J_n^y\}$ to be non-negative. Negative J_n^z then corresponds to ferromagnetic interactions.

In the absence of randomness, there are only two parameters in the problem: the ratios of the J's. For later convenience, we chose the asymmetric parametrization

$$\Delta \equiv 1+\delta = \frac{2J^z}{J^y+J^x} \tag{1.2}$$

and

$$a \equiv \frac{J^x - J^y}{J^y+J^x} \ . \tag{1.3}$$

The well-known phase diagram,[12] shown in Fig. 1 has quasi-long-range-ordered critical phases along the line $J^y = J^x$, $|J^z| < J^x$ (and other lines related to this by interchange of x, y, and z and sign changes to preserve J^y, $J^x \geq 0$); phases with long-range ferro- or antiferromagnetic order (with special lines along which there are no spin fluctuations in the ground state, such as large negative J_z with $-J^z > J^x$, J^y); and two special points with Heisenberg symmetry: $J^x = J^y$, $J^z = \pm J^x$.

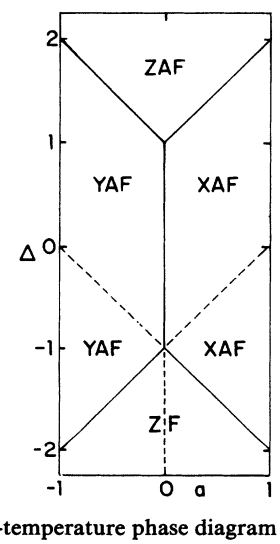

FIG. 1. Zero-temperature phase diagram of a pure spin-$\frac{1}{2}$ antiferromagnetic spin chain as a function of the anisotropy parameters $\Delta \equiv 2J_z/(J_x+J_y)$ and $a \equiv (J_x - J_y)/(J_x+J_y)$. The solid lines are phase boundaries on which the correlations decay as power laws with continuously variable exponents. On the dashed lines, there are no quantum fluctuations in the ground state. The point $\Delta = 1$, $a = 1$ is a Heisenberg antiferromagnetic while $\Delta = -1$, $a = 0$ can be transformed into a Heisenberg ferromagnet.

In the remainder of this section, we consider the effects of weak randomness. In Sec. II, the general renormalization-group transformation is introduced and used to analyze some of the properties of the random-singlet phase that occurs for the random XX chain at low temperatures. Section III is devoted to further study of random XY chains, including the effects of anisotropy and the transition from X-ordered to Y-ordered phases. In Sec. IV, the properties of XXZ antiferromagnetic chains which have conserved S_T^z are studied. In particular, the properties of phase transitions from random-singlet to Ising (Z) antiferromagnetic phases are analyzed. Finally, the results and open questions are summarized in Sec. V. Detailed analysis of the RG fixed flows and fixed points are relegated to the Appendix.

B. XY chain with weak randomness

An immediate question is: which of these phases are stable to small amounts of randomness in the exchange? We shall focus on the behavior along the lines $\delta = -1$, the XY chain, and $a = 0$, the XXZ chain. Stability of other parts of the phase diagram can be similarly analyzed; the main features are well exhibited by the two cases analyzed here.

We first consider adding randomness to the pure symmetric XX chain, which has quasi-long-range order. Analysis of the long-wavelength low-energy effective action by Doty and Fisher [2] showed that this point is *unstable* both to symmetric randomness in the $\{J_n^\perp = J_n^x = J_n^y\}$ and to random anisotropy [i.e., $a_n \equiv (J_n^x - J_n^y)/(J_n^x + J_n^y)$ random]. The nature of the resulting quasilocalized phases are analyzed in Sec. III. They can exhibit novel properties, including—rather surprisingly for a localized phase—power-law decay of the average correlation functions.

In contrast, the antiferromagnetically ordered phase for $J^x > J^y$ (or vice versa) is *stable* to weak bounded randomness due, essentially, to the existence of a gap in this phase. Nevertheless, we shall see that stronger randomness in the $\{J_n^x\}$ and $\{J_n^y\}$ will destroy the gap and concommitantly the "interfacial" tension between the two equivalent antiferromagnetic states, but the long-range order will be preserved. As a function of the mean $\bar{a}$ (or other measure) of the anisotropy distribution, there will be a phase transition from an antiferromagnetically ordered state with a staggered magnetization in the X direction to one with staggered magnetization in the Y direction. The nature of the phase transition and anomalous properties of the ordered phases will be analyzed in Sec. III. [Note that if the distribution of the exchanges alternates from one bond to the next, a *phase* with no staggered magnetization can occur (rather than just a line), as it does in the pure case with alternating exchange couplings.[13] In this paper we will restrict consideration to translationally invariant distributions and thus not consider such possibilities.]

C. *XXZ* chain with weak randomness

In the presence of weak exchange randomness that preserves the *XY* symmetry, the quasi-long-range-ordered phase of the pure system for $|J^z| < J^{\perp}$ is destroyed except for the segment on the ferromagnetic side $-1 \le \Delta = 1+\delta < -\frac{1}{2}$, which is *stable* to *weak* exchange randomness, but destroyed by stronger randomness. In particular, the quasi-long-range-ordered Heisenberg antiferromagnetic point, $\delta=0$, is destroyed by exchange randomness that preserves the Heisenberg symmetry: i.e., with all $\delta_n=0$ but J_n random. The resulting quasilocalized phases with *XY* symmetry are analyzed in Sec. IV.

As for the *XY* case, the long-range-ordered phases are *stable* to weak randomness, but their nature can be changed by stronger randomness. As a function of *uniform* anisotropy, δ, we thus expect a transition at $\delta=0$ from a quasilocalized *XX* phase to a phase with Ising antiferromagnetic order in the *Z* direction, the critical point exhibiting full Heisenberg symmetry. If the anisotropy is *random*, on the other hand, the phase transition will still occur but will *not* have Heisenberg symmetry. These transitions are analyzed in Secs. IV C and IV D. The conservation law of S_T^z makes the universality class for these quantum Ising transitions different from that of the random transverse field Ising chain analyzed previously, which has *no* conservation laws.

At the opposite end of the *XX* phase, i.e., large negative J^z, there will be a transition to an Ising *Z* ferromagnet. This transition will not be investigated in this paper as it appears to have a rather different character, that is not amenable to treatment by the methods used here.

II. RENORMALIZATION-GROUP TRANSFORMATION AND RANDOM-SINGLET PHASES

In this section we introduce a generalization of the renormalization-group transformation of Dasgupta and Ma.[8] The basic strategy is to first pick the largest coupling in the system. If the local ground state of the part of $\mathcal{H}$ involving this coupling is nondegenerate and the gaps to local excited states are larger, then the effects of the neighboring couplings can be treated perturbatively, yielding a new effective Hamiltonian with fewer degrees of freedom. (We will later need to generalize this to cases where the local ground state is degenerate due to symmetry.)

To be concrete, we attempt to decimate in this way a general *XYZ* chain by picking the bond with the largest J_n's; we will later be more precise about how this is defined. Denote the strongest bond $n=2$ with exchange couplings J_2^α and the exchanges on the bonds on either side J_1^α and J_3^α. The ground state of the local Hamiltonian

$$\mathcal{H}_{2-3} = \sum_\alpha J_2^\alpha S_2^\alpha S_3^\alpha \tag{2.1}$$

is a singlet provided $J_2^x + J_2^y$, $J_2^x + J_2^z$, and $J_2^y + J_2^z$ are all positive. We will restrict consideration here to this case. We can now attempt to treat the couplings J_1^α and J_3^α perturbatively. The effective Hamiltonian for the four low-lying states of the 1-2-3-4 chain that correspond to $S_1^z = \pm\frac{1}{2}$, $S_4^z = \pm\frac{1}{2}$, can be written in the form

$$\tilde{\mathcal{H}}_{1-4} = C + \sum_\alpha \tilde{J}_{14}^\alpha \tilde{S}_1^\alpha \tilde{S}_4^\alpha \tag{2.2}$$

with, to lowest order in J_1^α and J_3^α,

$$\tilde{J}_{14}^x \approx \frac{J_1^x J_3^x}{J_2^y + J_2^z} \tag{2.3}$$

and similarly for $\tilde{J}_{14}^{y,z}$. We will generally ignore the constant term in Eq. (2.2) which would, however, be needed to obtain the ground-state energy. If J_1^α and J_3^α are much less than J_2^α, then the operators $\tilde{S}_{1,4}$ are essentially $S_{1,4}$ up to $O(J_{1,3}/J_2)$ corrections. If all $\{J_{1,3}^\alpha\} \ll \{J_2^\alpha\}$, we can drop the tildes on $S_{1,4}$. Then Eq. (2.3) for $\tilde{J}_{14}^\alpha$ is a very good approximation and the effective Hamiltonian, Eq. (2.2), will yield the correct ground-state, low-energy spectrum, and low-temperature correlation functions of S_1 and S_4. The recursion relation Eq. (2.3) for the effective couplings is the basis of all the RG transformations that we will use.

In order for the perturbative expansion that yielded Eq. (2.3) to be a good approximation, we need the energy gaps to the other states of $\mathcal{H}_{2-3}$ to be large compared to the perturbations $J_{1,3}^\alpha$. The gaps of the local Hamiltonian, Eq. (2.1), are $\frac{1}{2}(J_2^x+J_2^y)$, $\frac{1}{2}(J_2^x+J_2^z)$, and $\frac{1}{2}(J_2^y+J_2^z)$; these appear in the denominators of the $\tilde{J}_{14}^\alpha$ in Eq. (2.3). Thus, the perturbation expansion will be good provided that at *least two* of the $\{J_2^\alpha\}$ are *large*, but will fail if only one of the $\{J_2^\alpha\}$ is large compared to the $\{J_{1,3}^\alpha\}$. With this condition, which will play an important role later, in mind, we proceed with the decimation transformation by picking the strongest bond among the set of $\tilde{J}_{14}$ and the other J_n with $n \neq 1$, 2, or 3. Note that the $\tilde{J}_{14}^\alpha$ are less than the J_2^α, thus $\tilde{J}_{14}$ will in all likelihood not be decimated away until a later stage.

A crucial feature of the transformation is that $\tilde{J}_{14}$ is *not correlated* with its new neighbors J_0 and J_5; thus the independence of the J_n's for different n will be preserved by the RG transformation. As the decimation proceeds, however, the distribution of the effective $\tilde{J}_n^\alpha$ (we renumber the sites for simplicity of notation and put tildes on all the remaining J's) will be modified and we must keep track of the joint distribution $P(\tilde{J}^x, \tilde{J}^y, \tilde{J}^z; \Omega)$ at energy scale Ω that corresponds to the largest remaining coupling in the system. The decimation will generate a flow equation for P as Ω is decreased

$$\frac{\partial P}{\partial \Omega} = R[P] , \tag{2.4}$$

where R is a complicated functional of P. In later sections, we will consider distributions of various combinations of the $\tilde{J}$'s and be more precise about how the strongest bond is defined.

A. *XX* chain

For now, we consider the simple case of the *XX* chain with

$$J_n^x = J_n^y \equiv J_n \tag{2.5}$$

and $J_n^z = 0$. The recursion relation is then simply

$$\tilde{J}^z = 0 ,$$
$$\tilde{J} = \frac{\tilde{J}_1 \tilde{J}_3}{\tilde{J}_2} , \tag{2.6}$$

where we have added tildes to all the J's since the transformation is iterated. The chain clearly remains an isotropic *XX* chain. The definition of the strongest bond is now trivial and we define

$$\Omega = \max\{\tilde{J}\} . \tag{2.7}$$

The form of the recursion relation suggests immediately transforming to logarithmic variables and we define

$$\Gamma \equiv -\ln\Omega \tag{2.8}$$

and

$$\zeta \equiv \ln(\Omega/\tilde{J}) \tag{2.9}$$

so that $\zeta \geq 0$ and *large* ζ corresponds to *small* J. The recursion relation then becomes

$$\tilde{\zeta} = \zeta_1 + \zeta_3 - \zeta_2 = \zeta_1 + \zeta_3 \tag{2.10}$$

since $\zeta_2 = 0$ because $\tilde{J}_2 = \Omega$ by choice of the strongest bond. For the distribution $\rho(\zeta,\Gamma)d\zeta$ of ζ at scale Γ, we then have

$$\frac{\partial\rho(\zeta,\Gamma)}{\partial\Gamma} = \frac{\partial\rho}{\partial\zeta} + \rho(0,\Gamma)\int_0^\infty d\zeta_- \int_0^\infty d\zeta_+ \delta(\zeta-\zeta_+-\zeta_-)\rho(\zeta_+,\Gamma)\rho(\zeta_-,\Gamma) , \tag{2.11}$$

where the $\partial\rho/\partial\zeta$ term arises from the change in the definition of ζ in Eq. (2.9) as Ω is decreased, and $\rho(0,\Gamma)d\Gamma$ is the fraction of bonds with ζ in the range 0 to $d\Gamma$, corresponding to $\tilde{J}$ in the range Ω to $\Omega(1-d\Gamma)$.

The form of the recursion relation, Eq. (2.10), implies that after a large fraction of the bonds have been decimated, the remaining $\ln\tilde{J}$ will be the sums and differences of large numbers of $\{\ln J_n\}$ of the bonds that have been decimated away between the remaining spins. Thus, we should expect the distribution of $\ln\tilde{J}$ and hence ζ to become broad. This behavior was found by Dasgupta and Ma[8] who studied the *XXX* case which is very similar to the *XX* case, as we shall see later.

A natural approach is to look for fixed point solutions of the RG flow equations by rescaling the ζ by an appropriate power of Γ. We thus try the transformation

$$\rho(\zeta,\Gamma) = \frac{1}{\Gamma} Q(\zeta/\Gamma,\Gamma) \tag{2.12}$$

and

$$\eta = \zeta/\Gamma , \tag{2.13}$$

yielding

$$\Gamma\frac{\partial Q}{\partial\Gamma} = Q + (1+\eta)\frac{\partial Q}{\partial\eta} + Q(0,\Gamma)\int_0^\eta d\eta' Q(\eta',\Gamma)Q(\eta-\eta',\Gamma) . \tag{2.14}$$

We then look for fixed points $Q^*(\eta)$ which are independent of Γ so that the left-hand side of Eq. (2.14) is zero. This fixed point equation has a one-parameter family of solutions parametrized by $Q_0^* \equiv Q^*(0)$. As shown in the Appendix, almost all of these have a power-law tail $Q^*(\eta) \sim 1/\eta^x$. Analysis of the flow equation, Eq. (2.14), shows that such power-law tails are preserved by the flow and cannot be generated. They correspond to distributions of J's,

$$P_0(J) \sim \frac{1}{J|\ln J|^x} , \tag{2.15}$$

which are extremely singular at small J. The low-energy behavior of chains with such singular distributions of exchanges is dominated by the weakest links yielding behavior somewhat different than that studied here.

In addition to these singular fixed points, there is a special fixed point with $Q_0^* = 1$ and

$$Q^*(\eta) = \theta(\eta)e^{-\eta} . \tag{2.16}$$

This corresponds to

$$P(\tilde{J},\Omega) = \frac{\alpha}{\Omega}\left[\frac{\Omega}{\tilde{J}}\right]^{1-\alpha}\theta(\Omega-\tilde{J}) \tag{2.17}$$

with

$$\alpha = \frac{1}{\Gamma} = -1/\ln\Omega \tag{2.18}$$

[where we have suppressed the dependence on the initial energy scale Ω_I which will enter via $\ln\Omega \rightarrow \ln(\Omega/\Omega_I)$].

Note that without the change of variables, Eq. (2.13) is not a fixed point, but it is of the form guessed by Dasgupta and Ma, who found that for small α, Eq. (2.17) is "almost" a fixed point. The sense in which this is correct is made precise by the rescaling and resulting fixed point Eq. (2.16) modified by corrections to scaling arising from irrelevant operators, which vanish for asymptotically low energies. The stability of the fixed point Eq. (2.16) is demonstrated in the Appendix.

In light of the approach of the distribution of $\ln\tilde{J}$ to the very broad distribution associated with the fixed point, we can reexamine the validity of the approximations made in the RG decimation. For a distribution of the form Eq. (2.17), the probability that one of the neighbors of the strongest bond with $\tilde{J} = \Omega$ has $J > C\Omega$ for some $C < 1$ is $1 - C^{2\alpha} \approx 2\alpha\ln(1/C)$ for small α. Thus, as the decimation proceeds, the probability that the lowest-order perturbative expression for the effective Hamiltonian Eq. (2.6) is *not* good decreases as $\alpha \approx 1/\Gamma$ and becomes asymptotically zero at the fixed point. Furthermore, when Γ increases by a factor of 2 (corresponding to a huge $e^{-\Gamma}$ fold decrease in Ω), the fraction of "bad" decimations is of order $1/\Gamma$. This strongly suggests that, provided one can get safely through the initial regime where the distribution of $\ln J$'s is not broad, the renormalization-group transformation will become exact asymptotically.

The initial relevance of weak randomness at low energies found from field-theoretic methods (Sec. I B) suggests that, for *any* nontrivial distribution of J's, the XX system will flow at low energies into the basin of attraction of the strong randomness fixed point. Although ruling out effects of errors in the RG decimation and development of correlations between the J_n's is difficult, comparison of the results we obtain with exact results on XX chains [3] and other cases discussed later strongly support this conjecture.[14] We will thus proceed on the basis of this conjecture and analyze its consequences.

B. Random-singlet phase

From the form of the decimation procedure, the nature of the resulting phase of the random XX chain should be clear: it is very similar to that found by Dasgupta and Ma[8] for the XXX case. At low energies, the system consists of pairs of spins which are coupled together into singlets over arbitrarily long distances, as shown schematically in Fig. 2. It has thus been dubbed a "*random-singlet phase.*"[10] The long singlet bonds are typically much weaker than the short ones and the singlet bonds cannot cross. If the distribution of the bare exchange couplings were narrow, then the physics at energies of order the initial J's would cause the spin-$\frac{1}{2}$ objects which make up the low-energy singlets to be spread out over a number of lattice sites, however at long-length scales the picture would still be the same.

The first question which we must address is how to determine the relation between energy and length scales, which should yield the strengths of the long bonds. This is simplest to do by calculating the fraction of spins n_Γ which are left at a given energy scale $\Omega = e^{-\Gamma}$. When Γ is increased by $d\Gamma$, a fraction $2\rho(0,\Gamma)d\Gamma$ of the spins left at scale Γ are decimated since there are equal numbers of couplings and spins and each decimated coupling removes two spins and replaces three couplings by one effective coupling. Since near the fixed point $\rho(0,\Gamma)=Q(0,\Gamma)/\Gamma \approx Q_0^*/\Gamma$, we have

$$\frac{dn}{d\Gamma}=\frac{-2Q_0^*}{\Gamma}n \tag{2.19}$$

implying that

$$n_\Gamma \approx \frac{1}{\Gamma^{2Q_0^*}}=\frac{1}{\Gamma^2} . \tag{2.20}$$

The typical distance between the remaining spins is thus

$$L_\Gamma \sim \frac{1}{n_\Gamma} \sim \Gamma^2 \sim [\ln(1/\Omega)]^2 . \tag{2.21}$$

We will later analyze the distribution of the bond lengths.

The result that $\Gamma \sim \sqrt{L}$ could perhaps have been anticipated: each $\ln\tilde{J}$ is a sum, with alternating signs, of a series of $\ln J_n$. If there were no correlation between which spins remained at scale Γ and the J_n's appearing in the sum, the sum would be an asymptotically Gaussian random variable with mean zero and variance $L[\overline{(\ln J)^2}-(\overline{\ln J})^2]$, i.e., $\Gamma \sim \sqrt{L}$. The way the decimation proceeds *changes* the *distribution* of the $\ln\tilde{J}$ but *preserves* the $\sqrt{L}$ *scaling.*

One immediate consequence of the scaling of lengths with energy is the form of the susceptibility at low temperatures. As long as $\Omega \gg T$, the excitations of the decimated pairs of spins will only be weakly excited by thermal fluctuations and can be ignored. When $\Omega \ll T$, on the other hand, all the remaining spins are coupled with $\tilde{J}$s $\ll T$ so that they are essentially free and will contribute a Curie term to the magnetic susceptibility in any direction. Most of the activity at low energies takes place on an exponentially broad distribution of energy scales so that to logarithmic accuracy we can just stop the decimation at scale $\Omega = T$ and find the susceptibility

$$\chi_\perp \sim \chi_z \sim \frac{n_{\Gamma_T}}{T} \sim \frac{1}{T[\ln(\Omega_I/T)]^2}\left[1+O\left(\frac{1}{\ln T}\right)\right] , \tag{2.22}$$

where $\Gamma_T \approx [\ln(\Omega_I/T)]$ and the error terms come from energy scales of order T and possibly from other sources.[15]

The result Eq. (2.22) for χ_z has been found previously[3] using the exact solvability of the XX chain via mapping it to free fermions. In particular, from an elegant argument, Eggarter and Riedinger[3] derived the form for the density of states of the fermions

$$N(E) \sim \frac{1}{|E|}\ln^3\left(\frac{1}{|E|}\right) \tag{2.23}$$

from which Eq. (2.22) follows by integrating over energies up to $E \sim T$. To the best of the author's knowledge, the result for $\chi_\perp$ is new. It is less natural in the fermion representation due to the nonlocal mapping from $S^{x,y}$ operators to Fermi operators. The agreement of the $\chi_z(T)$ behavior found here with the exact results lends support to the procedure used here and also to its generality for all well-behaved distributions of J_n's.

Some information on the spin correlations in the ground state can be readily gleaned from the RG. Provided that the effective spin-$\frac{1}{2}$ objects at low energies

FIG. 2. A schematic of the random-singlet ground state. Each spin forms a singlet pair with another spin indicated by the connecting "bond" lines. Most pair with nearby spins, but pairs with arbitrarily long distances separating the two spins also exist. Note that the bonds do not cross each other.

have finite extent (which we will argue below is the case) the long-range bonds imply that *some pairs* of widely separated spins have *strong* $O(1)$ correlations. The probability that a given pair of spins S_i and S_j form a singlet pair is proportional to the probability that both are not yet otherwise engaged at the energy scale Γ_{ij} at which $L_{\Gamma_{ij}} \sim |i-j|$. Since the probability that i survives until Γ and j survives until Γ are roughly independent until $\Gamma \sim \Gamma_{ij}$, the probability that both survive is roughly $n_{\Gamma_{ij}}^2 \sim |i-j|^{-2}$. If both survive until this scale, there is a good chance that they will form a singlet pair. The resulting *rare singlet pairs,* which are strongly correlated, yield lower bounds for the mean correlations and, as we shall argue below, actually *dominate* the *mean correlations.* Thus, we conclude that

$$\overline{C_{ij}} \equiv \overline{\langle \mathbf{S}_i \cdot \mathbf{S}_j \rangle} \sim \frac{(-1)^{i-j}}{|i-j|^2} . \tag{2.24}$$

Surprisingly, we have found power-law decay of the mean correlations in this disordered localized phase. The decay is faster than in the absence of randomness, for which $|\langle S_i \cdot S_j \rangle| \sim |i-j|^{-1/2}$, and is due to completely different physics: the effects of *rare correlations of local spins* rather than the effects of long-wavelength spin-wave-like excitations.

The correlations between *typical* pairs of widely separated spins in the random-singlet phase are, in contrast, very weak. A typical pair of widely separated spins, ij, will have a spin between them, say n, which was decimated at a scale Γ_n of order, say, $\Gamma_{ij}/2$. When this decimation occurred, the spin S_n became strongly correlated with one of the other remaining spins (which was one of its effective neighbors at scale Γ_n), but only very weakly correlated to its other effective neighbor at scale Γ_n. This is because the coupling to the weak-side neighbor is smaller by a factor of order $e^{-k\Gamma_n}$ with k of $O(1)$ but varying from one scale-Γ_n spin to another. This weak effective coupling induces correlations only of the same order. The spin S_n thus can only "transmit" correlations with magnitude of order $e^{-k\Gamma_n}$ from its weak-side effective neighbors. This implies that the correlation between S_i and S_j will be no larger than this; indeed on a logarithmic scale, it will, in fact, be *dominated* by the lowest-energy scale involved and thus be of order $e^{-k\Gamma_{ij}}$ with a somewhat different $O(1)$ coefficient k in the exponential.

Thus, we conclude that *typically,*

$$-\ln|C_{ij}| \sim \Gamma_{ij} \sim |i-j|^{1/2} \tag{2.25}$$

for large $|i-j|$. Indeed, we conjecture that $-\ln|C_{ij}|/(i-j)^{1/2}$ *converges in distribution* to a nontrivial distribution for large $|i-j|$. The rare pairs which dominate the average $\overline{C_{ij}}$ will be in the negligible-weight tail of the distribution for large $|i-j|$; these need not, indeed do not, scale as Eq. (2.25). This extreme difference between average and typical correlations is a hallmark of randomness dominated phases; it is especially pronounced in quantum systems.[16]

C. Distribution of bond lengths

The heuristic arguments presented above for the probability of finding long singlet bonds can be placed on a firmer footing by directly calculating the distribution of bond lengths l at a log-energy scale Γ. The recursion relation for the new bond lengths when bond "2" is decimated is very simple, merely

$$\tilde{l} = l_1 + l_2 + l_3 . \tag{2.26}$$

This must be combined with the recursion relation for ζ, Eq. (2.10), to obtain the needed distribution. Naively, since the recursion relations for $\tilde{\zeta}$ and $\tilde{l}$ are not directly coupled, one might have expected the renormalized $\{l\}$ and $\{\zeta\}$ to be independent at each stage of the renormalization. This is *not,* in fact, the case: If a renormalized bond has an atypically large ζ, it is likely to have arisen from adding up an atypically large number of ζ_n's, i.e., to be in a region where more bonds have been decimated away. This implies that it will also have atypically large l. Thus, we expect that ζ and l will be positively correlated. Note, however, that the independence of *different* renormalized bonds is still maintained. We thus must analyze the joint distribution $\rho(\zeta,l;\Gamma)d\zeta dl$ of ζ and l at scale Γ, treating, for simplicity, l as a continuous variable.

From the recursion relations, we find that

$$\frac{\partial\rho(\zeta,l;\Gamma)}{\partial\Gamma} = \frac{\partial\rho(\zeta,l;\Gamma)}{\partial\zeta} + \int_0^\infty dl_1 \int_0^\infty dl_2 \int_0^\infty dl_3 \int_0^\infty d\zeta_1 \int_0^\infty d\zeta_3 \delta(\zeta-\zeta_1-\zeta_3)\delta(l-l_1-l_2-l_3) \times\rho(0,l_2;\Gamma)\rho(\zeta_1,l_1;\Gamma)\rho(\zeta_3,l_3;\Gamma) . \tag{2.27}$$

For convenience, we introduce the simpler notation for convolutions over l, or ζ and l, $\underset{l}{\otimes}$ and $\underset{l\zeta}{\otimes}$, respectively. Equation (2.27) then becomes

$$\frac{\partial\rho}{\partial\Gamma} = \frac{\partial\rho}{\partial\zeta} + \rho(0,\cdot) \underset{l}{\otimes} \rho \underset{l\zeta}{\otimes} \rho \tag{2.28}$$

with the "$\cdot$" in $\rho(0,\cdot)$ denoting the dummy variable (l_2) to be convoluted in Eq. (2.27). As in the absence of l, we again look for fixed points by rescaling

$$\eta = \zeta/\Gamma \quad \text{and} \quad \lambda = l/\Gamma^\kappa \tag{2.29}$$

and adjust κ to find well-behaved fixed points. From the fact that the fraction of spins remaining is $n_\Gamma \sim \Gamma^{-2}$, we anticipate that $l \sim \Gamma^2$ so that

$$\kappa = 2 . \tag{2.30}$$

Rescaling, we look for distributions of the form

$$\rho(\zeta,l)=\frac{1}{\Gamma^3}Q(\zeta/\Gamma,l/\Gamma^2)=\frac{1}{\Gamma^3}Q(\eta,\lambda) \quad (2.31)$$

with

$$\Gamma\frac{\partial Q}{\partial \Gamma}=3Q+(1+\eta)\frac{\partial Q}{\partial \eta}+2\lambda\frac{\partial Q}{\partial \lambda}+Q(0,\cdot)\underset{\lambda}{\otimes} Q \underset{\lambda\eta}{\otimes} Q \quad (2.32)$$

with the $\eta(\partial/\partial\eta)$ and $\lambda(\partial/\partial\lambda)$ terms arising from $\partial\rho/\partial\Gamma$. Here we have dropped the explicit Γ dependence of Q and ρ; fixed points have no such dependence, i.e.,

$$\Gamma\frac{\partial Q}{\partial \Gamma}=0 . \quad (2.33)$$

Laplace transforming in λ to

$$\hat{Q}(\eta,\tilde{y})\equiv\int_0^\infty e^{-\tilde{y}\lambda}Q(\eta,\lambda)d\lambda \quad (2.34)$$

we have the fixed point equation

$$\hat{Q}+(1+\eta)\frac{\partial\hat{Q}}{\partial\eta}-2\tilde{y}\frac{\partial\hat{Q}}{\partial\tilde{y}}+\hat{Q}(0,\tilde{y})\hat{Q}(\cdot,\tilde{y})\underset{\eta}{\otimes}\hat{Q}(\cdot,\tilde{y})=0 . \quad (2.35)$$

After some exploration, a solution of the following form can be guessed:

$$\hat{Q}(\eta,\tilde{y})=e^{A(\tilde{y})+2\eta\tilde{y}(dA/d\tilde{y})-\eta} . \quad (2.36)$$

This requires that A satisfy

$$-2\tilde{y}\frac{dA}{d\tilde{y}}-4\tilde{y}^2\frac{d^2A}{d\tilde{y}^2}+e^{2A}-1=0 \quad (2.37)$$

with, since

$$\hat{Q}(\eta,\tilde{y}=0)=Q^*(\eta)=e^{-\eta} , \quad (2.38)$$

the boundary condition that

$$A(\tilde{y}=0)=0 , \quad (2.39)$$

which fixes A up to an overall scale change in $\tilde{y}$ that corresponds to the overall length scale. After choosing this scale for convenience, Eq. (2.37) has the solution

$$A(\tilde{y})=\tfrac{1}{2}\ln\tilde{y}-\ln\sinh\sqrt{\tilde{y}} \quad (2.40)$$

yielding

$$\hat{Q}(\eta,\tilde{y})=\frac{\sqrt{\tilde{y}}}{\sinh\sqrt{\tilde{y}}}e^{-\eta\sqrt{\tilde{y}}\coth\sqrt{\tilde{y}}} . \quad (2.41)$$

Integrating over η and writing

$$\tilde{y}=\Gamma^2 y , \quad (2.42)$$

we thereby obtain for the distribution of bond lengths l at scale Γ,

$$\Pr(l;\Gamma)=\int_{c-i\infty}^{c+i\infty}\frac{dy}{2\pi i}\frac{e^{ly}}{\cosh\Gamma\sqrt{y}} . \quad (2.43)$$

From the nearest singularity to the origin in the complex y plane, we see that for large $l\gg\Gamma^2$,

$$\Pr(l;\Gamma)\sim e^{-(\pi^2/4\Gamma^2)l} . \quad (2.44)$$

We must now ask whether the fixed-point distribution $\hat{Q}$ of Eq. (2.41) is stable and whether other fixed points exist. In the Appendix, the flows and fixed-point condition are analyzed in detail and it is concluded that the fixed point found above is the only fixed point which can arise with the initial l_n's being equal (or distributed with a finite mean), and the absence of a power-law tail in the ζ distribution. Other fixed points with different κ do also exist, however, these correspond to the very singular distributions of J, Eq. (2.15), mentioned earlier.

D. Finite-temperature correlations

The distribution of bond lengths at scale Γ gives information on the correlation functions at finite temperatures. If the renormalization is stopped when

$$\Gamma=\Gamma_T=\ln(\Omega_I/T) , \quad (2.45)$$

the longest existing singlet bonds will dominate the mean correlation function $\bar{C}_{ij}$ for large $|i-j|$. The longest bonds that have formed will form at the last stages when $\Gamma\leq\Gamma_T$. The distribution of these corresponds to $\eta\approx0$ in Eq. (2.41) so that

$$\bar{C}_{ij}(T)\sim\Pr\left[\text{bond length}=l=|i-j|\ \middle|\ \text{bond formed at scale }\Gamma_T\right]$$
$$\approx\int_{c-i\infty}^{c+i\infty}\frac{dy}{2\pi i}\frac{\Gamma_T\sqrt{y}\,e^{ly}}{\sinh(\Gamma_T\sqrt{y})}\sim e^{-\pi^2 l/\Gamma_T^2}\sim e^{-|i-j|/\xi_T} \quad (2.46)$$

for $|i-j|\gg\Gamma_T^2$, yielding the *thermal correlation length*

$$\xi_T\sim\left[\ln\frac{\Omega_I}{T}\right]^2 \quad (2.47)$$

with a nonuniversal coefficient that depends on the behavior at scales $\leq\Omega_I$. Note that this is *not* the correlation length that might have been expected from a simple analysis in terms of the free-fermion representation of the *XX* chain: That would have suggested a correlation length $\tilde{\xi}_T$ of order the "localization length" (defined by the Lyapunov exponent) at energy $E\sim T$ yielding [3]

$$\tilde{\xi}_T\sim\ln\frac{\Omega_I}{T} . \quad (2.48)$$

One expects that the correlation length of Eq. (2.48) will determine the "typical" correlations, i.e.,

$$\frac{-\ln C_{ij}(T)}{|i-j|} \to \frac{1}{\xi_T} \quad \text{with probability one} \tag{2.49}$$

(Ref. 17). Again, as at zero temperature, the mean correlations are dominated by very atypical pairs of spins that form anomalously long bonds with energies $\geq T$.

III. *XY* CHAIN

In this section, we begin to consider the effects of anisotropy by studying the properties of the random *XY* chain with Hamiltonian

$$\mathcal{H} = -\sum_n (J_n^x S_n^x S_{n+1}^x + J_n^y S_n^y S_{n+1}^y) \tag{3.1}$$

for various distributions of J_n^x and J_n^y. In the *XY* case, we can rotate some of the spins so as to make all the interactions *ferromagnetic*, and we have done so and chosen the opposite sign convention to earlier so that all the J_n^μ are positive and ferromagnetic. This is more convenient for analyzing the *X*- or *Y*-ordered phases which now become ferromagnetic. If alternate spins are rotated by 180° about the *z* axis, the results for the antiferromagnetic case can be recovered trivially.

We will consider distributions of the J_n^μ for which the $\{J_n^\mu\}$ are independent for different bonds, but may be correlated on the same bond, i.e., J_n^x and J_n^y are *not* independent. The most obvious way to proceed with the decimation RG is to choose the largest of the full set of $\{J_n^\mu\}$, say J_2^x and decimate the corresponding bond. The perturbative recursion relations are

$$\tilde{J}^x = \frac{J_1^x J_3^x}{J_2^y}$$

and (3.2)

$$\tilde{J}^y = \frac{J_1^y J_3^y}{J_2^x}$$

If the distributions are broad, then the perturbative expansion is good for $\tilde{J}^y$ because of the large denominator, but may be *bad* for $\tilde{J}^x$ if $J_2^y < J_1^x$ or $J_2^y < J_3^x$. Physically, this is because the spins S_1 and S_2, coupled by J_2, can have nearly degenerate ground states $|\rightrightarrows\rangle$ and $|\leftleftarrows\rangle$ (with the spins quantized in the *x* direction) with a splitting $\frac{1}{2}J_2^y$ between the odd (singlet) ground-state combination of these and the even combination of them. We will later see that in some cases, this problem can be handled by a somewhat different route, however the present approach will not work unless, with high probability, *both* J_2^x *and* J_2^y are $\gg J_1^x$, J_1^y, J_3^x, and J_3^y. This will be valid if the *J*'s are broadly distributed, but the anisotropies

$$a_n \equiv \frac{J_n^x - J_n^y}{J_n^x + J_n^y} \tag{3.3}$$

are, in an appropriate sense, small.

A. Weak anisotropy

We thus first consider the effects of weak anisotropy, a_n. It will be convenient to define the local anisotropy on a logarithmic scale by

$$\alpha_n \equiv \ln(J_n^x/J_n^y) = \ln\left[\frac{1+a_n}{1-a_n}\right] \tag{3.4}$$

and

$$J_n \equiv \sqrt{J_n^x J_n^y} \tag{3.5}$$

with

$$\zeta_n \equiv \ln(\Omega/J_n) \tag{3.6}$$

and

$$\Omega \equiv \max J_n \ . \tag{3.7}$$

The recursion relations, Eq. (3.2), become

$$\tilde{J} = \frac{J_1 J_3}{J_2} \tag{3.8}$$

so that

$$\tilde{\zeta} = \zeta_1 + \zeta_3 \ , \tag{3.9}$$

and

$$\tilde{\alpha} = \alpha_1 + \alpha_2 + \alpha_3 \ . \tag{3.10}$$

Although the recursion relations for ζ and α are separate, correlations will develop between them (as for ζ and l in the previous section), since the magnitudes of *both* are affected by the number of bonds which have been decimated to obtain a particular $\tilde{\zeta}$ and $\tilde{\alpha}$. If the distribution of α is much narrower than the distribution of ζ, which will obtain at least at intermediate energies if the anisotropy is initially very weak, then the perturbative expansion of Eqs. (3.2) is good and it does not make a substantial difference whether the largest J_n or the largest J_n^μ is chosen to be decimated. We must in any case keep track of the joint distribution $\rho(\zeta,\alpha;\Omega)$ of ζ and α; again within the perturbative approximation, the (ζ_n,α_n) pairs will be independent for different (renormalized) bonds n. Note that the pair of RG equations (3.9) and (3.10) are identical to those analyzed earlier, Eqs. (2.10) and (2.25), for the bond lengths.

B. Uniform anisotropy

If all the α_n's are the same sign, corresponding to uniform anisotropy, then the behavior will be similar to that of the bond lengths. Thus, the renormalized anisotropies α will scale as $\bar{\alpha}\Gamma^2$ with $\bar{\alpha}$ the mean bare anisotropy. When α becomes of order Γ, the width of the $\ln(\tilde{J}^x/\tilde{J}^y)$ distribution becomes of order that of the $\ln\tilde{J}^x$ distribution and the perturbative approximation breaks down. At this point, for $\bar{\alpha} > 0$ most of the J^x's will be bigger than most of the J^y's (or vice versa for $\bar{\alpha} < 0$) and the system will start to show long-range order in S^x, with the $\{S_n^x\}$ joining together to form spin clusters as discussed in more detail below. The correlation length associated with the resulting *X*-ferro–*Y*-ferro transition at the isotropic point $\bar{\alpha}=0$ scales as the crossover scale Γ^2, yielding

$$\xi_A \sim \frac{1}{|\bar{\alpha}|^{\nu_A}} \tag{3.11}$$

with $\nu_A = 2$. The resulting spontaneous magnetization

$$\overline{\langle S^x \rangle} \sim \bar{\alpha}^{\beta_A} \tag{3.12}$$

is determined by the number of spins remaining at this scale which is of order $1/\xi_A$ implying

$$\beta_A = \nu_A = 2 \ . \tag{3.13}$$

This might have been anticipated from the behavior of the spin correlations at the isotropic transition point. From scaling, we expect for $\bar{\alpha}$ small and r large

$$\overline{\langle S_0^x S_r^x \rangle} \sim \frac{1}{r^2} f_{\pm}(r/\xi_A) \tag{3.14}$$

with, for $\bar{\alpha} > 0$, $f_+ \sim (r/\xi_A)^2$ for large r yielding $\beta_A = \nu_A$. Although, as we shall see below, this X-Y transition is related to that of the random transverse field Ising spin chain analyzed previously,[11] it is in a different universality class, as can be seen from the different exponent β. The full crossover from isotropic random singlet to X (or Y) ferromagnetically ordered phases is difficult to analyze by the present methods, although it may be possible using the Ising decomposition discussed below.

C. Weak random anisotropy

If the α_n are random in sign with a *symmetric* distribution corresponding to statistical rotational symmetry, then the symmetry of the distribution must be preserved by the RG flows. Thus, we must find another, symmetric, fixed point of the recursion relations Eqs. (3.9) and (3.10). From the general analysis in the Appendix, we see that the naive expectation that the α_n's add roughly like random variables yields the correct scaling (although not the correct distribution due to the correlations between the $\tilde{\alpha}$'s and $\tilde{\zeta}$'s). The width of the distribution, σ_α, grows as $\sqrt{l_\Gamma} \sim \Gamma$ which is the same growth as the width of the (one-sided) distribution of ζ. Thus, if we rescale all ln$J$'s with Γ, the *random anisotropy is* seen to be *marginal.*

In principle, one might try to perform a calculation valid to higher order in the α's to try and determine whether random anisotropy is marginally relevant, irrelevant, or truly marginal. This would entail handling correctly the formation of spin clusters when, e.g., $J_2^x \gg J_1^y, J_3^y$ but $J_2^y \ll J_1^x, J_3^x$ so that the perturbative recursion relations, Eq. (3.2), break down. This might be possible via the decomposition method used below, but it is likely to be rather complicated and we have not attempted to carry this out. At this point, then, the behavior for weak random anisotropy is unclear. We shall see in the next subsection, however, that for strong random XY anisotropy the behavior is definitely distinct from the isotropic XX case.

D. Strong random anisotropy

We now turn to the opposite limit of strong random XY anisotropy. The simplest case to analyze is where the J_n^x and J_n^y are *independently* random with either the same distribution corresponding to statistical rotational symmetry, or slightly different distributions corresponding to the effects of a weak uniform anisotropy in addition to the strong random anisotropy. In this limit, the RG decimation procedure used so far breaks down and a different decimation analysis is needed.

To do this it is useful to divide the XY chain into two decoupled transverse field Ising chains. For notational convenience, we number the *bonds* in the original chain by n and the spins $S^\mu_{n+1/2}$. We then define two sets of Pauli spin matrices, as follows:

$$\begin{aligned}
\sigma_{2n}^x &= \prod_{j=1}^{2n} (2S_{j-1/2}^x) \ , \\
\sigma_{2n}^y &= 4S_{2n-1/2}^y S_{2n+1/2}^y \ , \\
\tau_{2n+1}^x &= \prod_{j=1}^{2n+1} (2S_{j-1/2}^x) \ , \\
\tau_{2n+1}^y &= 4S_{2n+1/2}^y S_{2n+3/2}^y \ .
\end{aligned} \tag{3.15}$$

This transformation is illustrated in Fig. 3.

The inverse transformation is

$$\begin{aligned}
S_{2n+1/2}^x &= \tfrac{1}{2}\sigma_{2n}^x \tau_{2n+1}^x \ , \\
S_{2n-1/2}^x &= \tfrac{1}{2}\tau_{2n-1}^x \sigma_{2n}^x \ , \\
S_{2n+1/2}^y &= \tfrac{1}{2}\bar{\tau}_{2n}^y \bar{\sigma}_{2n+1}^y = \frac{1}{2}\prod_{j=1}^{n} \tau_{2j-1}^y \sigma_{2j}^y \ , \\
S_{2n-1/2}^y &= \tfrac{1}{2}\bar{\sigma}_{2n-1}^y \bar{\tau}_{2n}^y = \frac{1}{2}\tau_1^y \prod_{j=2}^{n} \sigma_{2j-2}^y \tau_{2j-1}^y \ ,
\end{aligned} \tag{3.16}$$

where we have introduced dual variables $\bar{\sigma}$, $\bar{\tau}$,

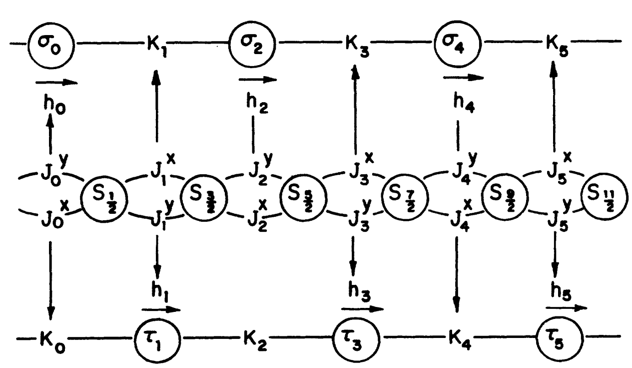

FIG. 3. Illustration of the transformation from an X-Y spin chain, shown in the center, to two decoupled Ising spin chains. The couplings J_{2n+1}^x and J_{2n}^x of the X-Y spin chain become, respectively, the couplings K_{2n+1} and K_{2n} between $\sigma_{2n}^z \sigma_{2n+2}^z$ and $\tau_{2n-1}^z \tau_{2n+1}^z$. The couplings J_{2n}^y and J_{2n+1}^y become, respectively, transverse fields $h_{2n}\sigma_{2n}^x$ and $h_{2n+1}\tau_{2n+1}^x$.

$$\begin{aligned}
\bar{\sigma}^x_{2j+1} &= \sigma^x_{2j}\sigma^x_{2j+2} ,\\
\sigma^y_{2j} &= \bar{\sigma}^y_{2j-1}\bar{\sigma}^y_{2j+1} ,\\
\bar{\tau}^x_{2j} &= \tau^x_{2j-1}\tau^x_{2j+1} ,\\
\tau^y_{2j+1} &= \bar{\tau}^y_{2j}\bar{\tau}^y_{2j+2} .
\end{aligned} \tag{3.17}$$

The Hamiltonian becomes

$$\mathcal{H} = -\sum_n [K_{2n}\tau^x_{2n-1}\tau^x_{2n+1} + h_{2n+1}\tau^y_{2n+1} + K_{2n+1}\sigma^x_{2n}\sigma^x_{2n+2} + h_{2n}\sigma^y_{2n}] \tag{3.18}$$

with

$$K_n = \tfrac{1}{4}J^x_n \tag{3.19}$$

and

$$h_n = \tfrac{1}{4}J^y_n .$$

We can alternatively write $\mathcal{H}$ in terms of the dual variables $\bar{\sigma}$, $\bar{\tau}$ whereupon $\bar{K}_n = \frac{1}{4}J^y_n$ and $\bar{h}_n = \frac{1}{4}J^x_n$, the duality thus manifesting the symmetry between X and Y.

The Hamiltonian, Eq. (3.18), is the sum of two *decoupled* random transverse field Ising chains. There can be decimated separately, by the procedure developed in Ref. [11]. The largest of the set of the $\{h_{2n+1}, K_{2n}\}$ is decimated. If a large h is decimated, a τ spin is eliminated and an effective new bond formed coupling second-nearest neighbors. If instead a large K is decimated, a *spin-cluster* is formed, which acts like a "super spin" with magnetic moment, $\tilde{m}$, equal to the sum of the moments of the two spin-cluster components that have been joined together by the decimation so that $\tilde{m}$ is the number of undecimated "active" spins in the cluster. The σ spins are handled similarly.

The recursion relation when, e.g., h_1 is decimated is

$$\tilde{K} = \frac{K_0 K_2}{h_1} \tag{3.20}$$

coupling spin 1 to spin 3. If K_2 is decimated

$$\tilde{h} = \frac{h_1 h_3}{K_2} \tag{3.21}$$

and

$$\tilde{m} = m_1 + m_3 \tag{3.22}$$

with the effective transverse (Y) field $\tilde{h}$ acting to flip the spin cluster which has moment $\tilde{m}$ in the X direction.

The RG recursions relations for J^μ can be seen to be identical to those found directly for the XY chain with an important difference: since we are, in general, now decimating only "part" of each bond of the original XY chain at each step, the condition for validity of the new recursion relations is just that the decimated part of the bond be much stronger than the opposite part (i.e., X instead of Y or vice versa) of the neighboring bonds. This is in contrast to the more restrictive condition needed earlier that *both* parts (i.e., J^x *and* J^y) of the decimated bond be much greater than *both* parts of each of the neighboring bonds. Thus, the current decimation procedure is much more general and can, in principle, be used to handle general forms of XY anisotropy. For the isotropic case, the two chains are decimated in exactly opposite ways with a spin being decimated on the σ chain whenever the corresponding bond is decimated on the τ chain. In general, the decimations on the two chains will proceed separately, but, with correlations between J^x_n and J^y_n, they will *not* be independent and the analysis will be complicated, since the correlations of the XY chain will involve correlations of both the Ising chains.

In the limit of *independent* $\{J^x_n\}$ and $\{J^y_n\}$, the two chains can be decimated independently with the resulting correlation functions of the two chains being independent of each other. We focus on the XX correlations natural in the σ, τ variables. The Ising correlation function

$$I_{ij} \equiv \langle \sigma^x_i \sigma^x_j \rangle \tag{3.23}$$

will be small unless the two spins are active in the same spin cluster at some length scale; if they are, their correlations will be of order 1 (somewhat reduced by the small scale, high-energy fluctuations). Results for the mean $\bar{I}_{ij}$ have thereby been obtained in considerable detail elsewhere.[11] On the critical manifold of the Ising chain, which corresponds to the *statistically isotropic* manifold of the XY chain,

$$\bar{I}_{ij} \sim \frac{1}{|i-j|^{2-\phi}} \tag{3.24}$$

with

$$\phi = \frac{1+\sqrt{5}}{2} \tag{3.25}$$

the golden mean. This arises from the number of active spins, m, in a cluster at scale Γ (and length scale $\sim\Gamma^2$) growing as $m \sim \Gamma^{\phi}$.[11] For the XY chain with independent random anisotropy we therefore obtain

$$\overline{C_{ij}} = \overline{\langle S^x_i S^y_j \rangle} \sim (\bar{I}_{ij})^2 \sim \frac{1}{|i-j|^{4-2\phi}} \tag{3.26}$$

the *mean correlation function* being dominated by pairs of spins which are active in the same cluster in both the σ and τ chains. Note that $\overline{C_{ij}}$ thus decays more slowly than for the isotropic case, a somewhat surprising result since the system would appear to be more random and more disordered. Indeed, the mean correlations actually decay more slowly than in the *nonrandom XXX* chain (and the XXZ chain with J^z slightly less than J^y). The decay, Eq. (3.26), is slow enough that its Fourier transform, the structure factor $C(q)$, diverges at the antiferromagnetic wave vector.

From the Ising chain analysis, we can also deduce the behavior in the presence of a small amount of mean bias, $\bar{\alpha}$, of the anisotropy. For $\bar{\alpha} > 0$, the system has long-range ferromagnetic order in the X direction with a correlation length for small $\bar{\alpha}$

$$\xi_A \sim \frac{1}{|\bar{\alpha}|^{\nu_A}} \tag{3.27}$$

with $\nu_A = 2$ similar to the behavior near the isotropic fixed point. The spontaneous X magnetization behaves in a different way, however, with exponent

$$\beta_A=\tfrac{1}{2}(4-2\phi)\nu_A=3-\sqrt{5}\ . \tag{3.28}$$

In this independent J^x and J^y case, one can also analyze the correlation functions and other properties from the equivalent Ising results. In particular, one can show explicitly that the mean correlation function does indeed decay exponentially with a correlation length ξ_A.[11]

In principle, one could analyze the effects of weak correlations between the J_n^x and J_n^y to see if they grow or shrink under renormalization. This would help resolve the question of what happens between the random isotropic XX fixed point and the independently random statistically isotropic fixed-point analyzed above; a fixed line with continuously variable exponents or a flow towards one or the other of these two fixed points are the simplest, although by no means the only, scenarios. We leave this for future investigation.

E. Comparison with exact results

So far, we have analyzed spin chains which are equivalent to noninteracting Fermi systems. Because of the nonlocal nature of the Jordan-Wigner transformation, however, extracting spin correlations from the fermion representation is notoriously difficult and most of the results we have obtained are new. Nevertheless, comparison with some of the few known exact results are useful to check our inexact method to see that it does, as claimed, yield exact universal properties at low energies and long-length scales.

As mentioned previously, the result for the low-temperature susceptibility of the XX chain agrees with earlier results.[3] A far more sensitive check involves comparisons with exact calculations of McCoy's[16] for a semi-infinite random transverse field Ising chain. He obtained the mean boundary magnetization

$$\overline{M_B(H_B)}=\overline{\langle\sigma_0^x\rangle} \tag{3.29}$$

as a function of a boundary field H_B in the X direction, which acts only on spin 0. As shown elsewhere,[11] this function can be computed in the scaling limit (near to the transition in small field) by our method. The whole resulting *function* agrees, up to nonuniversal coefficients, with the scaling limit extracted from McCoy's results. The *distribution* of $\ln M_B(H_B=0)$ in the ordered phase near the critical point[11] also agrees with McCoy's results confirming the validity of our approach for calculating typical as well as average behavior.

One of the advantages of the present method is that its success (or failure) does not depend on the free-fermion nature or even on solvability in any other known sense. It can thus also be applied to systems, as we shall now see, for which almost nothing can be computed exactly.

IV. *XXZ* CHAINS

We now turn to an analysis of the interesting random XXZ antiferromagnetic chains for which the Z component of the total magnetization S_T^z is conserved due to the rotational invariance about the Z axis.

A. *XXX* chain

The random antiferromagnetic Heisenberg (or XXX) chain, analyzed by Dasgupta and Ma,[8] behaves very similarly to the XX chain discussed above. The primary difference is that the recursion relation becomes

$$\tilde{J}=\frac{J_1J_3}{2J_2} \tag{4.1}$$

when the strong bond "2" is decimated.

On a logarithmic scale, on which the distribution of $\ln J$ becomes broad, the extra additive $\ln\frac{1}{2}$ that modifies the $\tilde{\zeta}$ recursion relation Eq. (2.10) becomes negligible at large scales and the fixed point has the *same form* as the XX case. The qualitative properties of the phase are also similar except that $\chi_\perp/\chi_z$, which is nonuniversal for the XX case, will of course be exactly one for the Heisenberg case.

At this point, it would be natural to guess that there will be a fixed line for the XXZ chain running from the XXX point to the XX point, and perhaps beyond. As we shall now see, this is *not* the case: random planar (XY) anisotropy about the Heisenberg point is relevant and the system flows at long scales to the XX fixed point.

B. Weak J^z coupling

We first show that weak S^zS^z interactions are irrelevant about the isotropic random XX fixed point. The recursion relations are

$$\tilde{J}^z=\frac{J_1^zJ_3^z}{2J_2^\perp} \tag{4.2}$$

and

$$\tilde{J}^\perp\approx\frac{J_1^\perp J_3^\perp}{J_2^\perp+J_2^z}\ , \tag{4.3}$$

where we see that for $J^z\ll J^\perp$, the $J^\perp$ recursion relation is approximately independent of J^z. Defining

$$\Delta_n\equiv\frac{J_n^z}{J_n^\perp} \tag{4.4}$$

we have

$$\tilde{\Delta}=\Delta_1\Delta_3\left[\frac{1+\Delta_2}{2}\right] \tag{4.5}$$

which become

$$\tilde{\Delta}\approx\frac{\Delta_1\Delta_3}{2} \tag{4.6}$$

for weak anisotropy. On a logarithmic scale, Eq. (4.6) is simply an additive recursion relation with a constant shift which will be negligible for the broad distributions that occur. The pair of recursion relation for

$$\zeta\equiv\ln(\Omega/J^\perp) \tag{4.7}$$

and $\ln\Delta$,

$$\tilde{\zeta}\approx\zeta_1+\zeta_3 \tag{4.8}$$

and

$$\ln\tilde{\Delta}\approx\ln\Delta_1+\ln\Delta_3$$

we have already encountered before, for the magnetic moments of spin clusters of the transverse field Ising chain at the critical point Eq. (3.22). We thus expect that the width of the distribution of $\ln\tilde{\Delta}$ grows as Γ^{ϕ}. Thus, the typical $\tilde{\Delta}$ vanishes as $e^{-c\Gamma^{\phi}}$, corresponding to, at length scale $l\sim\Gamma^2$, $\ln\tilde{\Delta}\sim -l^{\phi/2}$, so that *weak J^z coupling is strongly irrelevant* independent of its sign. (Note that this agrees with the intuition that interactions between fermions, which are proportional to J^z in the fermion representation of the *XXZ* chain, are irrelevant in a localized phase.) As we shall see below, however, strong J^z coupling is quite a different matter.

C. Weak anisotropy about the *XXX* chain

We may similarly analyze the behavior of weak anisotropy about the Heisenberg *XXX* fixed point. Defining

$$\delta_n\equiv\frac{J_n^z-J_n^\perp}{J_n^\perp} \tag{4.9}$$

and

$$\zeta_n\equiv\ln(\Omega/J_n^\perp)\ , \tag{4.10}$$

we have

$$\tilde{\delta}\approx\delta_1+\delta_3+\tfrac{1}{2}\delta_2$$

and

$$\tilde{\zeta}=\zeta_1+\zeta_3 \tag{4.11}$$

for small $\{\delta_n\}$. This case is intermediate between two of the cases analyzed previously. If the anisotropy is *uniform* so that all (or most) δ's are the same sign, then the methods of the Appendix yield a one-sided fixed-point distribution for δ with both mean and width growing as

$$\delta\sim\Gamma^{\lambda_U}\bar{\delta} \tag{4.12}$$

with $\bar{\delta}$ the initial mean anisotropy and

$$\lambda_U=\frac{1+\sqrt{7}}{2}\ . \tag{4.13}$$

At scale $\Gamma_U\sim|\bar{\delta}|^{-1/\lambda_U}$ the anisotropies become of order unity and Eq. (4.12) is no longer valid. Beyond this scale, there is an asymmetry between positive, uniaxial (Ising-like) and negative, planar (*XY*-like) anisotropy.

For planar anisotropy, the recursion relation Eq. (4.5), for $\Gamma\gg\Gamma_U$, becomes that for small Δ, Eq. (4.6), analyzed above and the system flows rapidly to the *XX* fixed point. Thus we see that the whole fixed line between the *XX* and *XXX* points of the pure system *collapses,* in the presence of randomness, to the random *XX* fixed point. For negative Δ, this collapse also occurs except in the case of weak randomness and $-1<\Delta<-\frac{1}{2}$ for which randomness is irrelevant and the quasi-long-range-ordered phase of the pure system persists;[2] and for $\Delta<-1$ where the system becomes ferromagnetic.

For uniaxial Ising anisotropy, the behavior is more interesting. Beyond the scale Γ_U, the system becomes strongly anisotropic but singlets will still form since with large J_2, we can have $J_2^z\gg J_2^\perp$ but still usually $J_2^\perp\gg J_1^z$, J_3^z since at scale Γ_U, $J_n^z\sim J_n^\perp$ but $J_2^\perp/J_1^\perp$ is typically of order e^{Γ_U}. In this intermediate regime we have

$$\tilde{J}^\perp\approx\frac{J_1^\perp J_3^\perp}{J_2^z}\ ,\qquad \tilde{J}^z\approx\frac{J_1^zJ_3^z}{2J_2^\perp}\ , \tag{4.14}$$

yielding, with

$$J_n\equiv\sqrt{J_n^\perp J_n^z}\ ,\qquad \tilde{J}\approx\frac{J_1J_3}{\sqrt{2}J_2}\ , \tag{4.15}$$

and

$$\tilde{\Delta}\approx\frac{\Delta_1\Delta_2\Delta_3}{2}\ , \tag{4.16}$$

so that for large $|\ln\Delta_n|$,

$$\ln\tilde{\Delta}\approx\ln\Delta_1+\ln\Delta_2+\ln\Delta_3\ . \tag{4.17}$$

A convenient definition of ζ is then

$$\zeta\equiv\ln(\Omega/J) \tag{4.18}$$

yielding Eq. (2.10) for ζ. These recursion relations are valid as long as the distribution of $\ln\Delta$ is much narrower than that of ζ. From the analysis of the addition of lengths in Sec. II C, we see that the width of the distribution of anisotropy becomes, for $\Gamma\gg\Gamma_U$,

$$\ln\Delta\sim\left[\frac{\Gamma}{\Gamma_U}\right]^2 \tag{4.19}$$

since the width is of order unity at scale Γ_U. The ζ distribution still has width $\sim\Gamma$. The process of singlet formation thus only breaks down when $\Gamma\sim\Gamma_X$ with $\ln\Delta(\Gamma_X)\sim\zeta(\Gamma_X)$ yielding

$$\left[\frac{\Gamma_X}{\Gamma_U}\right]^2\sim\Gamma_X \tag{4.20}$$

so that, from Eq. (4.11),

$$\Gamma_X\sim\frac{1}{\bar{\delta}^{2/\lambda_U}}\ . \tag{4.21}$$

This corresponds to a length scale $\sim\Gamma_X^2$ thereby yielding a correlation length for small initial Ising anisotropy $\bar{\delta}$,

$$\xi\sim\frac{1}{\bar{\delta}^{\nu}} \tag{4.22}$$

with

$$\nu=\frac{4}{\lambda_U}=\frac{8}{1+\sqrt{7}}\ . \tag{4.23}$$

Beyond this length scale, analogy with the transverse field Ising case suggests that the Z components of the remaining spins start grouping together into clusters leading to spontaneous staggered Z magnetization M_s^z of order the fraction of spins remaining active at scale ξ, i.e., for small positive anisotropy $\bar{\delta}$

$$\overline{M}_s^z \sim \bar{\delta}^{\beta} \tag{4.24}$$

with $\beta=\nu$. It may be possible to analyze this regime by a different decimation procedure, more analogous to reference,[11] but this has not yet been accomplished.

What we have found here is the behavior of the transition from an XX random-singlet phase through a Heisenberg random-singlet critical point to an Ising antiferromagnetically ordered phase as a function of anisotropy applied to an *initially isotropic* Heisenberg spin chain. In the next subsection, we consider the same transition in the more general case of random anisotropy for which the critical point does *not* have Heisenberg symmetry.

D. Random anisotropy *XXZ* chain

We now consider the general transition from an XX random-singlet phase to an Ising antiferromagnet as a function of random anisotropy that preserves the rotational invariance about the Z axis. Before doing this, we first show that the XXX fixed point is *unstable* to *random XXZ* anisotropy.

The recursion relations for weak anisotropy were derived above, Eqs. (4.11). We are now interested, however, in δ_n's which are random in sign. The recursion relations for weak anisotropy are symmetric in $\delta \leftrightarrow -\delta$ so we search for a scaling solution for the distribution of δ which is symmetric in δ (rather than the one-sided distribution relevant above). From the Appendix we see that such even distributions have width $\tilde{\sigma}_\delta$ which scales as

$$\tilde{\sigma}_\delta \sim \Gamma^{\lambda_R} \tag{4.25}$$

with

$$\lambda_R=\frac{1+\sqrt{6}}{4}\ . \tag{4.26}$$

Thus random anisotropy is relevant at the XXX random singlet fixed point. When the renormalized width $\tilde{\sigma}_\delta$ becomes of order unity, the weak anisotropy approximation breaks down. This occurs when $\Gamma \sim \Gamma_R \sim \sigma_\delta^{-1/\lambda_R}$ corresponding to a crossover length scale, in terms of the initial σ_δ,

$$l_R \sim \frac{1}{\sigma_\delta^{2/\lambda_R}}\ . \tag{4.27}$$

Beyond this length scale, or if the bare anisotropy is not small, the anisotropy renormalizes in a different, asymmetric, way. Defining

$$D \equiv \ln\Delta \equiv \ln(J^z/J^\perp)\ , \tag{4.28}$$

we have

$$\tilde{D} \approx D_1+D_3+\max(D_2,0) \tag{4.29}$$

when bond "2" is decimated. The condition for the validity of the recursion relation Eq. (4.29) is that the width of the D distribution, $\tilde{\sigma}_D$, remain much smaller than the width, Γ, of the distribution of $\zeta=\ln(\Omega/\tilde{J})$. [Note that only large *positive* D cause problems since they make the perturbative recursion relation for $\tilde{J}^z$, Eq. (4.1), fail.] Because of the nature of the recursion relation for $\tilde{\Delta}$, Eq. (4.29), the general methods of the Appendix cannot be used directly. Nevertheless, we can still search for scaling solutions for the distribution of D with width

$$\tilde{\sigma}_D \sim \Gamma^{\psi}\ . \tag{4.30}$$

Examination of the recursion relation Eq. (4.29) and our previous results immediately yields two scaling solutions: One of these only has support for positive D, so that the recursion relation becomes like that for the bond lengths and thus $\psi=\psi_+=2$. Likewise, another solution only has support for negative D so that Eq. (4.29) reduces to the form Eq. (3.22) for the moments of transverse field Ising spin clusters yielding $\psi=\psi_-=(1+\sqrt{5})/2$. These two fixed points are both stable. If we start with a distribution which has both positive and negative D_n's, it will generically flow to either one or the other of these. However, there must be a critical manifold in between which does not flow to either but instead to a *random anisotropy critical fixed point* in which we are interested. Although this fixed point has not been found analytically, a useful bound can be obtained for ψ.

Consider a more general recursion relation for the rescaled variable

$$\theta \equiv D/\Gamma^{\psi}\ , \tag{4.31}$$

$$\theta=\theta_1+\theta_3+\max(\theta_2,M)\ . \tag{4.32}$$

For $M=0$ this has the desired form of Eq. (4.29), while for $M \to -\infty$ the recursion relation simplifies to $\theta=\theta_1+\theta_2+\theta_3$. For any M, we expect that there will be a stable fixed point with most θ positive and one with most θ negative, as well as a critical fixed point separating the basins of attraction of these. For $M=-\infty$, the critical fixed point is found by the methods of the Appendix; it has $\psi(-\infty)=1$. Since changing M is not a singular perturbation, we expect $\psi(M)$ to be a continuous function of M. In the Appendix, we prove that for any finite nonpositive M, all fixed point distributions have

$$\text{either } \psi<1 \tag{4.33}$$

$$\text{or } \psi>\tfrac{1}{2}[1+(13-4\sqrt{5})^{1/2}]\approx 1.507\ , \tag{4.34}$$

and

$$\psi<\tfrac{1}{2}[1+(13+4\sqrt{5})^{1/2}]\approx 2.842\ .$$

For the critical fixed point at $M=0$ to be continuously connected to that at $M=-\infty$, it must thus have $\psi<1$ [the other, large ψ, domain of Eq. (4.34) includes both ψ_+ and ψ_-]. This implies that the width of the D distribution,

$$\tilde{\sigma}_D \sim \Gamma^{\psi} \ll \Gamma \tag{4.35}$$

so that the perturbative renormalization group remains *valid* at this random anisotropy critical fixed point.

If the mean anisotropy, $\overline{\delta}$, is varied from XY-like to Isinglike, the system will undergo a phase transition from an XX random-singlet phase to an Ising antiferromagnet at some critical value of anisotropy $\overline{\delta}_c$, which is, in general, not equal to zero. Near to this transition, the behavior will be controlled by the critical fixed point discussed above. We parametrize the distance from the transition by

$$\epsilon \equiv \overline{\delta} - \overline{\delta}_c \ . \tag{4.36}$$

On a logarithmic scale this corresponds roughly to taking $D_n \to D_n + \epsilon$. For small ϵ, the growth of the asymmetry of the distribution of random anisotropies will be controlled by the (unique) unstable eigenvalue, λ, about the critical fixed point distribution with the D scaled as Γ^{ψ}, i.e., the renormalized ϵ defined on a logarithmic scale, will grow as

$$\tilde{\epsilon} \sim \epsilon \Gamma^{\lambda+\psi} \ . \tag{4.37}$$

When $\tilde{\epsilon}$ becomes of order the (logarithmic) width $\tilde{\sigma}_D$ of the distribution at the critical fixed point Eq. (4.30), most of the distribution will become strongly asymmetric with D either mostly positive or mostly negative. This occurs when $\Gamma \sim \Gamma_\epsilon$ with

$$\Gamma_\epsilon \sim |\epsilon|^{-1/\lambda} \ . \tag{4.38}$$

Beyond this scale the anisotropies will grow with exponent $\psi_\pm$ depending on the sign of ϵ.

We first discuss the simpler behavior on the XX side of the transition. On scales beyond Γ_ϵ, the singlet pairs that form are primarily of XX character (which could be probed, in principle, by the anisotropy of local ac susceptibilities) but the variations of J from one pair to another are still much larger than the variations in the anisotropies. Beyond Γ_ϵ, the overall anisotropy grows as

$$\tilde{\epsilon} \sim -(\Gamma/\Gamma_\epsilon)^{\psi_-}\Gamma_\epsilon^{\psi} \tag{4.39}$$

and becomes of order Γ when $\Gamma \sim \Gamma_X$ with

$$\Gamma_X \sim \Gamma_\epsilon^{(\psi_- - \psi)/(\psi_- - 1)} \sim |\epsilon|^{-(\psi_- - \psi)/\lambda(\psi_- - 1)} \ . \tag{4.40}$$

Beyond this scale, the typical ratios of $\tilde{J}^z$ to $\tilde{J}^\perp$ on one bond is smaller than those of $\tilde{J}^\perp$'s from one bond to another, but since the ground states of pairs are singlets, this only affects the excited state spectrum in a subtle way, and the physics will not change much. Associated with the crossovers Γ_ϵ and Γ_X are crossover lengths which scale as Γ_ϵ^2 and Γ_X^2, but since the mean correlations are power laws in all regimes for $\epsilon < 0$ (and the typical correlations decay as $e^{-\sqrt{|i-j|}}$), there is no well-defined correlation length.

On the Ising side of the transition, the behavior is rather different. At scale Γ_ϵ, the singlets that form have predominantly Ising-like local excitations, but again the anisotropies are not enough to prevent the formation of singlets or to make the perturbative recursion relations break down. Beyond Γ_ϵ, the anisotropy grows with exponent $\psi_+ = 2$ so that

$$\tilde{\epsilon} \sim (\Gamma/\Gamma_\epsilon)^2 \Gamma_\epsilon^{\psi} \tag{4.41}$$

until $\tilde{\epsilon} \sim \Gamma$, which occurs for $\Gamma \sim \Gamma_I$ with

$$\Gamma_I \sim \epsilon^{-(2-\psi)/\lambda} \ . \tag{4.42}$$

At this scale, the log anisotropies are comparable to the width of the $\ln\tilde{J}$ distribution at which point the energy denominators in Eq. (4.1) can become smaller than the factors in the numerators and the perturbative approximation breaks down. Beyond this scale, the spins will, instead, start to pair up into superspin clusters and the broken Ising symmetry will manifest itself. The staggered magnetization, $\overline{M}_s^z$, should be of order the fraction of spins left at scale Γ_I, yielding the exponent for $\overline{M}_s^z$,

$$\beta = \frac{4-2\psi}{\lambda} \ . \tag{4.43}$$

Numerical analysis of the critical fixed point and small perturbations from it should enable one to calculate λ and ψ, and hence β; this has not yet been carried out.

In the Ising antiferromagnetic phase, it is not clear whether there is a true correlation length—i.e., exponential decay of mean truncated correlations—with

$$\xi \sim \Gamma_I^2 \tag{4.44}$$

which diverges as $\epsilon \to 0$ with exponent $\nu = \beta$, or whether ξ is only a crossover length. To answer this would entail understanding the decay of mean truncated correlations to the long distance value of $(\overline{M}_s^z)^2$ which we have not attempted to do. (Note that the analogous question can be addressed in the ordered phase of the transverse field Ising chain by the methods of Ref. 11.)

V. SUMMARY AND DISCUSSION

We have investigated in this paper the properties of various phases of random quantum spin chains and phase transitions between them. The main results can usefully be summarized in terms of renormalization-group flow diagrams for purely antiferromagnetic interactions at zero temperature.

A. XY antiferromagnets

When $J_z = 0$, antiferromagnetic and ferromagnetic chains are equivalent via a rotation of alternate spins. The results of Sec. IV can thus be directly carried over to the antiferromagnetic case. The anisotropies which favor X over Y are denoted $\{a_n\}$, as in Eq. (3.34), with the distribution of a_n's characterized by its mean $\overline{a}$ and width σ_a.

The zero-temperature RG flow diagram of random XY chains as a function of $\overline{a}$ and σ_a is shown in Fig. 4. Along the line $\overline{a} = 0$, the distribution of a is taken to be symmetric under $a \leftrightarrow -a$, i.e., $X \leftrightarrow Y$; this line is statistically isotropic with the point at the bottom of the line fully isotropic, i.e., all $a_n = 0$. The two stable fixed points XAF and YAF represent long-range-ordered antiferromagnetic phases with staggered magnetization

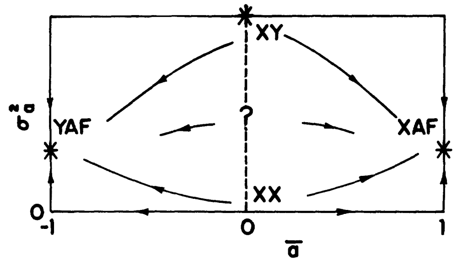

FIG. 4. Schematic renormalization group flow diagram of a random XY antiferromagnetic spin chain as a function of the mean anisotropy $\bar{a}$ and its variance σ_a^2, with the local anisotropy $a_n \equiv (J_n^x - J_n^y)/(J_n^x + J_n^y)$. For $\bar{a} > 0$, the system is an X antiferromagnet (XAF) while for $\bar{a} < 0$ it flows to the YAF fixed point. The XX random-singlet critical point with no anisotropy controls the transition for $\sigma_a = 0$. On the other hand, with J_n^x and J_n^y independently random, but identically distributed, the XY critical fixed point is obtained. Note that although this has power-law decay of mean correlations, it is *not* a random-singlet state. The flows on the phase boundary $\bar{a} = 0$ are not known; either a fixed line or flow to one of the two end points is possible.

$$\overline{M}_s^x = (-1)^n \overline{\langle S_n^x \rangle} \neq 0 \tag{5.1}$$

or

$$\overline{M}_s^y = (-1)^n \overline{\langle S_n^y \rangle} \neq 0 \;, \tag{5.2}$$

respectively. In general, in these antiferromagnetic phases there will *not* be an interfacial tension between the two states with opposite staggered magnetization because of the existence of arbitrarily weak renormalized couplings.

For weak *bounded* disorder and strong uniform anisotropy, on the other hand, the antiferromagnetic phases *can* have an interfacial tension, however, this will not occur if the mean anisotropy $\bar{a}$ is small. For sufficiently weak disorder, the antiferromagnetic staggered susceptibility, $\chi_s(T)$, will diverge exponentially at low temperatures in the antiferromagnetic phases. However generically, $\chi_s(T)$ will only diverge as a nonuniversal power of T; this effect has been analyzed in detail for the random transverse field Ising spin chain.[11]

Separating the two antiferromagnetic phases is a critical manifold, the line $\bar{a} = 0$ in Fig. 4, which is statistically isotropic, at least on long scales. Note that a crystal which has XY symmetry (i.e., a fourfold axis) in the absence of impurities will, in the presence of random impurities, generally be statistically isotropic and thus lie *on* the critical manifold. Anisotropic strain would give rise to a small mean anisotropy and could be used to tune through the XAF to YAF transition.

We have analyzed two limiting points on the critical manifold in detail. The fully isotropic point, labeled XX in Fig. 4 represents a *random-singlet phase* in which the low-energy picture of the system consists of every spin being paired into a singlet with some other spin. The bonds connecting the spin pairs have a distribution of lengths extending out to arbitrarily long range, a long bond corresponding to very weak coupling of the singlet pair. At zero temperature, the correlation function $C_{ij} = \langle S_i \cdot S_j \rangle$ *typically* decays as $e^{-k\sqrt{|i-j|}}$ with k random, in the sense that $-\ln|C_{ij}|/\sqrt{|i-j|}$ converges to some nontrivial distribution at large distances. Nevertheless, the *mean* correlations, which would be measured by, e.g., neutron scattering, are dominated by singlet pairs (ij) for which $-C_{ij} = O(1)$. These yield

$$\overline{C_{ij}} \sim \frac{(-1)^{i-j}}{|i-j|^{\eta}} \tag{5.3}$$

with $\eta = 2$.

At low temperatures, the excitations predominantly involve breaking of the weak long singlet bonds. The resulting nearly free spins each yield a Curie susceptibility with the result that

$$\chi_z(T) \sim \chi_x(T) \sim \frac{1}{T \ln^2(1/T)} \;. \tag{5.4}$$

Perhaps surprisingly, the staggered susceptibility diverges in just the same way as the uniform susceptibility; indeed, for frequencies $\omega \ll T$, the susceptibility $\chi'(q,\omega;T)$ is only weakly q dependent, due to the local nature of the dominant excitations. For $\omega \gg T$, on the other hand, singlet pairs will play a role and χ' will peak at the antiferromagnetic wave vector.

The isotropic XX random singlet phase is unstable to *uniform anisotropy,* yielding an antiferromagnetic phase with correlation length $\xi \sim \bar{a}^{-\nu_A}$, with $\nu_A = 2$, for decay of the *mean* correlations of the opposite type, i.e., S^yS^y correlations in the XAF phase. For small $\bar{a} > 0$, the staggered magnetization scales as $\overline{M}_s^x \sim \bar{a}^{\beta_A}$ with $\beta_A = 2$.

Within the critical manifold, small *random anisotropy* is found to be *marginal.* But it is not clear whether it is truly marginal so that a fixed line exists with continuously variable exponents, or whether nonlinear flows will make anisotropy in fact relevant or irrelevant. The simplest scenario, which the author suspects is correct, is that random anisotropy is marginally *relevant* with the flow towards the strongly random anisotropic fixed point denoted XY in Fig. 4; this might be resolvable by the techniques of Sec. III D and Ref. 11.

The other case that we have analyzed is the extreme case of J_n^x and J_n^y *independent* but identically distributed. The resulting statistically isotropic field point (XY in Fig. 4) is *not* a random-singlet phase; a spin can be strongly correlated with *many* spins far away. Nevertheless, many of its properties are similar: decay of the typical correlations as $e^{-\sqrt{i-j}}$; power-law decay of mean correlations [but here with exponent $\eta = 3 - \sqrt{5}$ and a concommitantly different power of $\ln(1/T)$ in the susceptibility]; and instability to weak uniform anisotropy with correlation exponent for small $|\bar{a}|$, $\nu_A = 2$, and staggered magnetization exponent $\beta_A = 3 - \sqrt{5}$.

We have not analyzed the stability of the independent J^x, J^y fixed point to small correlations between J_n^x and J_n^y on the same bond, but this might be possible. It would help to settle the question of the flow for intermediate random anisotropy raised above.

B. XXZ antiferromagnets

The other type of random spin chain that we have analyzed in detail is a chain with rotational invariance about the Z axis, so that $J_n^x=J_n^y\equiv J_n^\perp$ and the total Z magnetization, S_T^z, is conserved. The RG flow diagram is shown in Fig. 5 as a function of the mean and random uniaxial anisotropy $\overline{\delta}$ and σ_δ about the isotropic *Heisenberg* (*XXX*) system.

With only uniform anisotropy initially, the *XXZ* system exhibits two phases: the *XX* random singlet and the Ising antiferromagnet (ZAF) with staggered magnetization in the Z direction. Weak random or uniform J^z are irrelevant at the *XX* random-singlet fixed point (in contrast to the pure system in which J^z is exactly marginal; see Fig. 1). Generically, the ZAF phase has no interfacial tension (as discussed earlier for the somewhat different *X*AF and *Y*AF phases), but for weak bounded disorder and strong Z anisotropy, the interfacial tension will be nonzero.

Separating the *XX* random singlet and ZAF phases in the absence of random anisotropy is the isotropic Heisenberg *XXX* random-singlet phase, which is very similar to the *XX* random-singlet phase. The corresponding critical fixed point is unstable to uniform anisotropy with a somewhat complicated crossover to ZAF phase for positive $\overline{\delta}$. The staggered Z magnetization for small positive $\overline{\delta}$ vanishes as $\overline{M_s^z}\sim\overline{\delta}^{\beta}$ with

$$\beta=\frac{8}{1+\sqrt{7}} . \tag{5.5}$$

Note that this transition from ZAF to disordered is very different, due to the conserved S_T^z, from that of the random transverse field Ising system. In principle, it could be studied by anisotropically straining a system with Heisenberg symmetry, although it does not seem possible to avoid at least weak uniform or random anisotropies in a random one-dimensional or quasi-one-dimensional magnetic system.

More plausible is a system with almost perfect *XX* symmetry, but random uniaxial anisotropy along the Z direction parallel to the chains, and mean anisotropy varied by changing the pressure.[18] Random uniaxial anisotropy is *relevant* at the *XXX* random singlet fixed point, as shown in Fig. 5. If the mean anisotropy $\overline{\delta}$ is carefully tuned to a critical value $\overline{\delta}_c$, a new critical fixed point, *XXZC*, is reached. This again is a random-singlet point, but now with strong random anisotropy which, nevertheless, is *not* strong enough to prevent singlet formation dominating the low-energy physics. We have not found the fixed-point distributions for this *XXZC* point analytically, however, bounds can be placed on an important exponent, ψ, Eq. (4.30). The (unique) unstable eigenvalue, λ, about this critical fixed point will, together with ψ, determined how $\overline{M_s^z}$ vanishes as $\overline{\delta}\to\overline{\delta}_c$ from the ZAF phase. We leave for the future numerical study of the behavior near this fixed point.

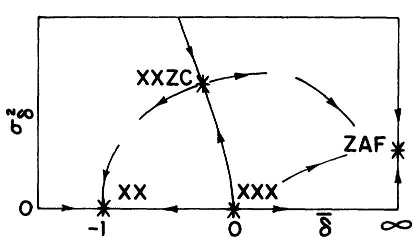

FIG. 5. Schematic renormalization-group flows for a random *XXZ* chain as a function of the mean anisotropy $\overline{\delta}$ and its variance σ_δ^2 with the local anisotropy $\delta_n\equiv 2J_n^z/(J_n^x+J_n^y)-1$. In the absence of anisotropy, the *XXX* random-singlet phase occurs. This fixed point controls the transition as a function of uniform anisotropy with $\sigma_\delta=0$; from an *XX* easy plane random-singlet phase to a Z (Ising) antiferromagnetic phase, ZAF. If the anisotropy is random, the transition is controlled by the *XXZC* critical fixed point.

C. Validity of results

The methods used here are by their nature approximate, but we have argued that they become exact at low energies and should apply whenever the Hamiltonian is in the basin of attraction of one of the fixed points studied. For the case of the *XY* random spin chain, results derived using the equivalence to free fermions can be used to check some of our results.[3] As mentioned earlier, a far more stringent test is the full boundary magnetization scaling function of the related random transverse field Ising chain analyzed elsewhere.[11,16] In these cases, a combination of the transfer matrix techniques used in the exact solutions and the present RG method should be possible. This could be done by explicitly working with the random transfer matrices $T_n(\omega)$ along the chain;[5,11] these are functions of frequency, corresponding to energy levels of the free-fermion problem. By choosing in which order to multiply the transfer matrices together (by finding the strongest effective couplings) and keeping track of the low-frequency behavior of the partial products, it should be possible to carry out the RG transformation much more systematically.[11] This has not been done in detail. What should make it work, however, is the observation that the low-frequency behavior of products of $T_n(\omega)$ can only be parametrized simply if they are multiplied in the order that corresponds to the decimation procedure we have carried out in this paper. Whether correlation functions, which are usually tricky to get from fermion methods, can actually be computed by such a transfer matrix RG procedure, we leave as an open question.

The power of the *present* method, of course, is that it does not in any way depend on the solvability or noninteracting fermion character of the spin chains: the random Heisenberg (*XXX*) chain, which is not known to be exactly solvable, is just as easy to analyze as the random *XX* chain. It is interesting to note that the solvability of the nonlinear integrodifferential fixed-point equations that arise here has nothing to do with the solvability of the underlying model in the *XX* case; it is an entirely separate, seemingly fortuitous, property of the simple iterative RG equations.

It may be possible to obtain rigorous bounds on correlation functions from the present approach for systems in which the initial distribution of couplings are very broad and the perturbative basis of the decimation RG becomes very good with high probability. At this point, however, we leave the results in a similar state to those of the Kosterlitz-Thouless theory of the 2D XY model: approximate, but yielding results which, if correct, are *exactly* correct.

D. Extensions

Various extensions of our results for random quantum spin chains may be possible. First, the behavior in a magnetic field, H, should be analyzable for some of the cases considered here, by means similar to that used for the random transverse field Ising chains.[11] The natural scaling variable will be $\ln H$ in an analogous way to the $\ln T$ behavior, that appears in, e.g., the low-temperature susceptibility, Eq. (2.22). Some information on scaling functions as functions of $\ln T$, $\ln H$, and, in some cases, distance to a critical point will be necessary to analyze any experimental or numerical data, since by necessity data will not be able to cover a wide range of length scales due to the logarithmic dependence of length scales on energy and hence on temperature.

For the most interesting transition studied here, the XXZ critical point with random anisotropy that separates, as a function of mean anisotropy, an Ising antiferromagnet and an XX random singlet phase, we have only obtained very limited information. The exponents should, however, be calculable numerically from the fixed-point equations. It may also be possible to follow the flow out to the Ising antiferromagnet fixed point and obtain information on this crossover, as has been done elsewhere for the random transverse field Ising transition.[11] This would, however, necessitate a controllable RG transformation which can handle both the formation of singlets and the formation of spin clusters with large staggered moments. Whether this is possible in this case is unclear; it should be possible, however, for the transition from X-ferro to Y-ferro phases by means of the transformation to two unoccupied (but in general, not independent) Ising transverse field chains that was used in Sec. IV.

The methods of this paper depend heavily on the nearest-neighbor nature of the interactions and the independence of the couplings from bond to bond. Nevertheless, it may be possible to treat weak second-neighbor interactions or weak correlations between the couplings perturbatively. Unfortunately, in general this would entail controlling the development of longer-range interactions and more complicated correlations under renormalization, and is hence likely to be extremely difficult.

Physically, we do not expect that weak correlations or second-neighbor interactions should dramatically affect the low-energy behavior: if each spin is involved in several couplings, we still expect the distribution of the effective couplings to be broad at low energies and hence the strongest remaining coupling to dominate. Thus, we conjecture that the phases and phase transitions studied here will still be controlled by the same fixed points and hence exhibit the same universal properties. (Note that for the random transverse field Ising system, weak short-range correlations in the couplings have indeed been shown to be irrelevant at the critical fixed point.[11])

Another interesting extension would be to higher spin chains, particularly spin 1. In the absence of randomness, a spin-1 antiferromagnetic chain with Heisenberg symmetry is in a disordered phase with a gap (the Haldane gap).[19] Because of the gap, this phase should be stable to weak randomness. For broadly distributed exchange couplings, on the other hand, a random-singlet phase can probably exist, as for spin $\frac{1}{2}$. Analysis of the decimation RG flows in this case will be complicated by the generation of biquadratic couplings, but the coupled recursion relations and fixed-point equations should be analyzable, at least numerically. The properties of such a spin-1 random-singlet phase will presumably be qualitatively similar to the spin-$\frac{1}{2}$ case. Whether there are additional intermediate phases for spin-1 Heisenberg chains, and the nature of other parts of the phase diagram, we leave for future investigation.

E. Higher dimensions

The most interesting open question is, perhaps: How much of the behavior found here persists, even qualitatively, in higher dimensions? In particular, are there quantum disordered phases and zero-temperature quantum phase transitions in two- and three-dimensional random quantum antiferromagnets which are similar to those in one dimension?

First, we should note that for weakly random exchange, antiferromagnetically ordered phases with broken continuous symmetry can surely exist in 2D and 3D at low temperatures. But, secondly, for strong randomness, random-singlet phases can also exist, as predicted by Bhatt and Lee,[10] and found experimentally in the insulating phase of Si:P.[20] In this system, the susceptibility is divergent at low temperatures, with $\chi \sim 1/T^{\alpha}$ over a reasonable range of T, but the form of the asymptotic behavior is not known; it is most likely similar to the 1D case, Eq. (2.22), but with a larger power of $\ln(1/T)$ in the denominator. (It has recently been predicted[21] that a random-singlet phase, albeit one with very weakly divergent susceptibility, is actually generic also in the *metallic* phase of Si:P, although in this case the experimental evidence and theoretical arguments are less convincing.)

The properties of 2D and 3D random-singlet phases have not been worked out in as much detail as in 1D, but it seems clear that they are qualitatively similar. The main questions, then, concern the existence of other zero-temperature phases and the nature of the quantum transitions between the various phases.

Restricting ourselves first to systems with Heisenberg symmetry, at least one other phase is possible in higher dimensions: a spin-glass phase can exist, at least at zero temperature, if the interactions are frustrated. In the absence of frustration, a transition from a Heisenberg antiferromagnetic phase to a random-singlet phase at zero temperature may well exist, although it is hard to definitively rule out an intermediate phase. If such a transition does exist, then it will be from an ordered phase to a phase with no long-range order but with infinite staggered susceptibility caused by rare local regions. This transition would thus, like the superfluid to Bose-glass transition of helium in porous media at zero temperature,[22] be very difficult to analyze starting from high dimensions, and indeed, may have no upper critical dimension. What its nature will be is unclear.

If a magnetic system only has XY symmetry, then a transition may be possible from an XX random-singlet phase to an Ising Z antiferromagnetic phase as a function of the mean anisotropy. Since this transition occurred already in 1D, one might expect that its character in higher dimensions would be similar. One might then ask whether the energy will scale exponentially with the length scale at the transition, as in 1D. This will presumably depend on whether or not the critical point is a random-singlet-like phase. If it is, then scaling like that in 1D may obtain. If not, then more conventional scaling is likely to obtain, albeit still with anomalous behavior of scaling functions caused by rare regions. Elsewhere,[11] it is argued that for the simple random transverse field Ising system, the disordered to ferromagnetic transition in $d>1$ will probably *not* be like that in 1D, since the effective interactions between far away spins need not pass through anomalously weak intervening effective bonds for $d>1$.

Whether our study of one-dimensional random quantum spin chains will give substantial insight into the behavior of quantum phase transitions in higher-dimensional random systems, or whether only the qualitative properties of random-singlet and other disordered phases will persist in higher dimensions, it is clear that the low-temperature behavior of random quantum systems is a very rich field. The effects of randomness—both via rare anomalous regions and on collective phenomena—are far greater than in classical random systems. It is hoped that in the near future, more experiments will become possible on these and other random quantum systems.

ACKNOWLEDGMENTS

I would like to thank the theoretical and statistical physics groups at the Ecole Normale Supérieure and the Perse Diaconis Summer Institute for hospitality during the time when much of this work was carried out. This work was supported in part by the NSF through Grant No. DMR 9106237 and via Harvard University's Materials Research Laboratory, and also by the Alfred P. Sloan Foundation.

APPENDIX

In this appendix, the general structure of the RG flows and fixed points are analyzed. Various results used in the text, particularly for the exponents describing the scaling of various quantities at fixed points, are derived.

As in the text, we consider the RG transformation generated by decimating the bonds with couplings J_n (which can be $J^\perp$, $\sqrt{J^\perp J^z}$ or other depending on the context); between the upper cutoff Ω and $\Omega-d\Omega$. On a logarithmic scale, we define

$$\zeta\equiv\ln(\Omega/J) \tag{A1}$$

so that ζ is non-negative and

$$\Gamma\equiv-\ln\Omega\ . \tag{A2}$$

If a bond, say "2", is decimated (so that $\zeta_2=0$), the recursion relation for ζ is

$$\tilde{\zeta}=\zeta_1+\zeta_3\ , \tag{A3}$$

where a constant additive part has been ignored, anticipating broad distributions of ζ for which such additive constants are irrelevant.

In addition, there may be one (or more) auxiliary variables with recursion relations

$$\tilde{x}=x_1+x_3+\Upsilon x_2 \tag{A4}$$

with Υ a fixed constant. For example, in the case of bond lengths, x becomes l and the coefficient $\Upsilon=1$.

The joint distribution $P(\zeta,x;\Gamma)d\zeta dx$ obeys the RG flow equation

$$\frac{\partial P(\zeta,x)}{\partial\Gamma}=\frac{\partial P(\zeta,x)}{\partial\zeta}+\int\int\int dx_1dx_2dx_3\int\int d\zeta_1d\zeta_3\delta(\zeta-\zeta_1-\zeta_3)\delta(x-x_1-x_3-\Upsilon x_2)P(0,x_2)P(\zeta_1,x_1)P(\zeta_3,x_3)\ , \tag{A5}$$

where we have not exhibited the dependence of P on Γ. The first term arises from the shift in ζ implicit in its definition, Eq. (A1), and the change in Ω. Note that with the support of ζ restricted to $\zeta\geq0$, the loss of total probability from the first term in Eq. (A5), $-P_0$, with

$$P_0\equiv\int P(0,x)dx\ , \tag{A6}$$

is exactly compensated by the increase from the second term, i.e., each strong decimated bond ("2") is replaced, although the neighboring bonds are not. Thus, the fraction of remaining bonds $n(\Omega)$ is decreased by $2P_0n$ from the loss of the neighboring bonds of the strong decimated bond. Thus, we have

$$\frac{dn}{d\Gamma}=-2P_0n\ . \tag{A7}$$

1. Fixed-point distribution of ζ

We first analyze the behavior of the distribution of ζ by itself: $P(\zeta)\equiv\int P(\zeta,x)dx$; which renormalizes as

$$\frac{\partial P}{\partial\Gamma}=\frac{\partial P}{\partial\zeta}+P_0 P\underset{\zeta}{\otimes}P\ . \tag{A8}$$

It is useful to consider the behavior of P for large ζ. If P decays more slowly than exponentially, then the large ζ behavior of the convolution $P\otimes P$ is dominated by regions of the integration in which one of the ζ' is small and the other $(\zeta-\zeta')$ is large. Thus, $P\otimes P$ has the same decay as P, but multiplied by a factor $2P_0$; the $\partial P/\partial\zeta$ term is thus negligible for large ζ. The form of a subexponential tail is therefore unchanged by renormalization, so if P decays exponentially or more rapidly initially, this property should be preserved by the flow. We thus search for fixed points that decay rapidly in a rescaled variable

$$\eta\equiv\zeta/\Gamma^{\kappa}\ . \tag{A9}$$

The rescaled distribution $Q(\eta)d\eta$ renormalizes as

$$\Gamma\frac{\partial Q}{\partial\Gamma}=\kappa\left[Q+\eta\frac{\partial Q}{\partial\eta}\right]+\Gamma^{1-\kappa}\left[\frac{\partial Q}{\partial\eta}+Q_0 Q\otimes Q\right] \tag{A10}$$

with $Q_0\equiv Q(\eta=0)$.

Fixed points, i.e., solutions to (A10) with no explicit Γ dependence, are dominated by the terms in the first bracket for $\kappa>1$, yielding the unphysical solution $Q=c/\eta$; or by the terms in the second bracket for $\kappa<1$, yielding (via Laplace transforms) a Q which oscillates in sign for large η and is thus also unphysical. Therefore, we must have $\kappa=1$ yielding Eq. (2.13). Physical fixed points are therefore solutions to

$$Q+\eta\frac{\partial Q}{\partial\eta}+\frac{\partial Q}{\partial\eta}+Q_0 Q\otimes Q=0\ . \tag{A11}$$

Laplace transforming to $\hat{Q}(z)$ yields

$$z\frac{\partial\hat{Q}}{\partial z}=z\hat{Q}+Q_0[\hat{Q}^2-1] \tag{A12}$$

with the constraint that

$$Q_0=Q(0)=\lim_{\eta\to 0+}\frac{1}{2\pi i}\int_{c-i\infty}^{c+i\infty}\hat{Q}(z)e^{z\eta}dz\ . \tag{A13}$$

We can linearize Eq. (A12) by the transformation

$$\hat{Q}=\frac{-z}{uQ_0}\frac{du}{dz} \tag{A14}$$

yielding

$$u''+\frac{1}{z}u'-u'-\frac{Q_0^2}{z^2}u=0\ , \tag{A15}$$

with primes denoting d/dz.

For small z, the two linearly independent solutions to Eq. (A15) behave as $u_{\pm}\sim z^{\pm Q_0}$. The normalization condition $\hat{Q}(0)=1$ forces some of the z^{-Q_0} solution to be included. We thus write

$$u=z^{-Q_0}v+Cu_{+} \tag{A16}$$

with $v\to$const for small z. We must now distinguish between whether or not $2Q_0$ is an integer. If $2Q_0\neq$ integer, then we have

$$v=\sum_{n=0}^{\infty}v_n z^n \tag{A17}$$

with

$$v_{n+1}=\frac{n-Q_0}{(n+1)(n+1-2Q_0)}v_n \tag{A18}$$

implying that for large (positive) z, $v(z)\sim z^{\alpha}e^{z}$, so that if $C=0$ in Eq. (A16), $\hat{Q}\approx -z/Q_0$ for large z which is unphysical; thus we conclude that there must be an admixture of the u_{+} solution, i.e., $C\neq 0$. This implies, however, that $\hat{Q}$ has a z^{2Q_0} singular part for small z which corresponds to a $1/\eta^{2Q_0+1}$ tail in $Q(\eta)$ which, as we argued above, cannot arise from an initially rapidly decaying $P(\zeta)$. Therefore, we must restrict consideration to $2Q_0=m=$integer. In general, this implies a $z^m\ln z$ part in v and hence in $\hat{Q}$ and again a $1/\eta^{2Q_0+1}$ tail in $Q(\eta)$. The only exception to this is if $m=2$, since in this case the series Eq. (A17) for v terminates and $v=1+z$.

Thus we conclude that we must have

$$Q_0=1\ . \tag{A19}$$

In this case, the general form for $\hat{Q}$ can be found explicitly:

$$\hat{Q}=\frac{1+C'e^{z}(1-z)}{1+z+C'e^{z}}\ . \tag{A20}$$

We see that only for $C'=0$ does this yield the correct large z behavior $\hat{Q}\approx Q_0/z$ corresponding to the discontinuity at $\eta=0$. The only well-behaved fixed point is thus simply $\hat{Q}=1/(1+z)$ yielding

$$Q^{*}(\eta)=e^{-\eta}\theta(\eta)\ . \tag{A21}$$

The stability of the solution, Eq. (A21), to perturbations which decay exponentially in η can be found by studying the linearized flow equation for $q\equiv Q-Q^{*}$

$$\Gamma\frac{\partial q}{\partial\Gamma}=q+(1+\eta)\frac{\partial q}{\partial\eta}+q_0\eta e^{-\eta}+2q\otimes e^{-\eta} \tag{A22}$$

with $q_0=q(0)$ and $\int q\,d\eta=0$ since Q is a probability distribution. Equation (A22) can be shown to have exactly one eigensolution $q(\eta,\Gamma)=q_{\lambda}(\eta)\Gamma^{\lambda}$ with $\lambda=-1$ and

$$q_{-1}(\eta)=(1-\eta)e^{-\eta} \tag{A23}$$

which can be seen to correspond to an irrelevant shift in the origin of Γ: $\Gamma\to\Gamma+\delta\Gamma$.

A general exponentially decaying perturbation q will, under renormalization, evolve into a more rapidly decaying q plus a multiple of q_{-1}, which decays away since $\lambda<0$. Thus, we conclude that Q^{*} is, indeed, a stable fixed point. (A more detailed analysis of flows such as that of Q is carried out in Ref. 11.)

2. Joint distribution with auxiliary variables

With the auxiliary variable x in Eqs. (A4) and (A5), we can again look for fixed points with rescaled variables η and

$$\chi \equiv x/\Gamma^{\psi} \ . \tag{A24}$$

The fixed-point equation for the joint distribution $Q(\eta,\chi)$ (dropping the * superscript) becomes

$$0=\Gamma\frac{\partial Q}{\partial \Gamma}=(1+\psi)Q+(1+\eta)\frac{\partial Q}{\partial \eta}+\psi\chi\frac{\partial Q}{\partial \chi}+\int d\chi_2 Q(0,\chi_2)\int\int d\chi_1 d\chi_3 Q(\cdot,\chi_1)\underset{\eta}{\otimes} Q(\cdot,\chi_3)\delta(\chi-\chi_1-\chi_3-\Upsilon\chi_2) \ , \tag{A25}$$

where the dots denote the dummy variables (η) of the convolution. The last term in Eq. (A25) can be written in the form

$$W \underset{\chi}{\otimes} Q \underset{\eta\chi}{\otimes} Q \ , \tag{A26}$$

where

$$W(\chi)\equiv\frac{1}{\Upsilon}Q\left[0,\frac{\chi}{\Upsilon}\right] \tag{A27}$$

which reduces to $W=\delta(\chi)$ for $\Upsilon=0$.

From Eq. (A28) it is straightforward to analyze the conditional moments

$$C_p(\eta)\equiv\langle\chi^p|\eta\rangle\equiv\frac{1}{Q(\eta)}\int\chi^p Q(\eta,\chi)d\chi \tag{A28}$$

which can be found iteratively in p from

$$-\psi p C_p-\eta C_p+(1+\eta)\frac{dC_p}{d\eta}+M_p(\eta)=0 \tag{A29}$$

with

$$M_0(\eta)=\eta \ ,$$
$$M_1(\eta)=W_1\eta+2C_1\otimes 1 \ , \tag{A30}$$
$$M_2(\eta)=W_2\eta+2C_2\otimes 1+4W_1C_1\otimes 1+2C_1\otimes C_1 \ ,$$

etc., where

$$W_p\equiv\int\epsilon^p W(\epsilon)d\epsilon=\Upsilon^p C_p(0) \ . \tag{A31}$$

We must now distinguish two cases, depending on whether or not the distribution of η is symmetric (even) in η.

3. Asymmetric case

In general, $C_1(\eta)$ will be nonzero. It satisfies the equation

$$-\psi C_1-\eta C_1+(1+\eta)\frac{dC_1}{d\eta}+2\int_0^{\eta}C_1(\eta')d\eta'+W_1\eta=0 \tag{A32}$$

or, differentiating

$$(1+\eta)\frac{d^2C_1}{d\eta^2}+(1-\psi-\eta)\frac{dC_1}{d\eta}+C_1+W_1=0 \tag{A33}$$

with the boundary condition

$$\frac{dC_1}{d\eta}(0)-\psi C_1(0)=0 \tag{A34}$$

and

$$W_1=\Upsilon C_1(0) \ . \tag{A35}$$

Equation (A33) has two linearly independent solutions: one is simply

$$C_1^a=1+\frac{\Upsilon+1}{\psi-1}\eta \tag{A36}$$

and the other

$$C_1^b\sim e^{\eta} \tag{A37}$$

for large η. The second solution is unphysical since it could only arise from an initial distribution with very large x's associated with large η's. Therefore, we must have $C_1\propto C_1^a$. The proportionality constant is just an overall scale factor (which is a redundant operator). We see, however, that C_1^a does not satisfy the required boundary condition Eq. (A34) unless

$$\psi(\psi-1)=\Upsilon+1 \tag{A38}$$

yielding

$$\psi_{\rm asym}=\tfrac{1}{2}(1+\sqrt{5+4\Upsilon}) \ . \tag{A39}$$

(The other solution with $\psi<0$ is unphysical, since the typical x must grow under renormalization.) It is not clear *a priori* that even with ψ given by Eq. (A39) there exists a well-behaved fixed point. We shall see, however, that in this case an explicit expression can be found for the fixed point which does indeed satisfy all the necessary conditions. Before showing this, we first analyze the case of a symmetric (in x) distribution.

4. Symmetric case

By symmetry in this case, $C_p(\eta)=0$ for odd p. We therefore study the conditional second moment, $C_2(\eta)$. From Eqs. (A29) and (A30), this satisfies

$$-2\psi C_2-\eta C_2+(1+\eta)\frac{dC_2}{d\eta}+W_2\eta+2\int_0^{\eta}C_2(\eta')d\eta'=0 \tag{A40}$$

with

$$W_2=\Upsilon^2 C_2(0) \ . \tag{A41}$$

This has the same form as Eq. (A32) with ψ replaced by 2ψ and Υ by Υ^2. Thus, the well-behaved solution becomes

$$C_2=1+\frac{\Upsilon^2+1}{2\psi-1}\eta \tag{A42}$$

with

$$\psi_{\rm sym}=\tfrac{1}{4}(1+\sqrt{5+4\Upsilon^2})\ . \tag{A43}$$

5. Fixed-point distributions

In order to find the actual fixed-point distributions $Q(\eta,\chi)$, we analyze the generating function for the conditional moments

$$\hat{C}(\eta,\omega)\equiv\int d\chi\, e^{i\omega\chi}Q(\eta,\chi)/Q(\eta) = \sum_{p=0}^{\infty}\frac{(i\omega)^p}{p!}C_p(\eta)\ , \tag{A44}$$

and

$$\hat{W}(\omega)=\int d\chi\, e^{i\omega\chi}W(\chi)=\hat{C}(0,\Upsilon\omega)\ . \tag{A45}$$

We then have the fixed-point condition

$$(1+\eta)\frac{\partial\hat{C}}{\partial\eta}-\eta\hat{C}-\psi\omega\frac{\partial\hat{C}}{\partial\omega}+\hat{W}\hat{C}\underset{\eta}{\otimes}\hat{C}=0\ . \tag{A46}$$

By studying the first few conditional moments $C_p(\eta)$ as above, a solution of the following form can be guessed:

$$\hat{C}=\exp\left[A(\omega)+\psi\eta\omega\frac{dA}{d\omega}\right] \tag{A47}$$

yielding

$$\hat{C}\underset{\eta}{\otimes}\hat{C}=\eta\exp\left[2A(\omega)+\psi\eta\omega\frac{dA}{d\omega}\right]\ . \tag{A48}$$

The terms in Eq. (A46) thus either have the η dependence of $\hat{C}$ or of $\eta\hat{C}$. The terms proportional to $\hat{C}$ yield

$$\psi\omega\frac{dA}{d\omega}-\psi\omega\frac{dA}{d\omega}=0 \tag{A49}$$

which is satisfied automatically [i.e., by the choice of the form of $\hat{C}$, Eq. (A47)] while the $\eta\hat{C}$ terms yield

$$\psi\omega\frac{dA}{d\omega}-\psi^2\left[\omega\frac{d}{d\omega}\right]^2 A+\hat{W}e^{A}-1=0 \tag{A50}$$

with

$$\hat{W}(\omega)=e^{A(\Upsilon\omega)}\ , \tag{A51}$$

and the boundary conditions

$$A(0)=0 \quad\text{and}\quad \omega\frac{dA}{d\omega}\bigg|_{\omega=0}=0 \tag{A52}$$

needed for normalization of the conditional probability distribution, $\hat{C}(\eta,\omega=0)=1$.

For the case $\Upsilon=1$, Eq. (A50) becomes a second-order ODE which can be solved with the appropriate boundary conditions, yielding

$$A(\omega)=\ln\{(k\omega)^{1/\psi}/\sinh[(k\omega)^{1/\psi}]\}\ , \tag{A53}$$

and

$$\psi\omega\frac{dA}{d\omega}=1-(k\omega)^{1/\psi}\coth[(k\omega)^{1/\psi}] \tag{A54}$$

with $\psi=1$ corresponding to the symmetric ease and $\psi=2$ the asymmetric case and k an integration constant. The necessity of one of these two values of ψ can be seen: if $2/\psi$ is not an integer, A (and hence, $\hat{C}$) has a branch cut at the origin, implying power-law decay of Q for large χ.

For the *symmetric case,* with $\Upsilon=1$, we have from Eq. (A43) $\psi=1$ and $\hat{C}(\eta,\omega)$ must be a real function of ω, implying k real and we can choose $k=1$ (the overall scale factor is arbitrary). The nearest singularity in the complex plane then occurs at $\omega=\pm i\pi$ so that for *any* fixed η and large χ,

$$C(\eta,\chi)\sim e^{-\pi\chi}\ . \tag{A55}$$

For this case

$$\hat{C}(\eta,\omega)=\frac{\omega}{\sinh\omega}e^{-\eta(\omega\coth\omega-1)} \tag{A56}$$

and hence

$$\hat{Q}(\eta,\omega)=\frac{\omega}{\sinh\omega}e^{-\eta\omega\coth\omega} \tag{A57}$$

yielding, on integrating over η and Fourier transforming in ω, the fixed-point distribution for χ alone,

$$Q(\chi)=\frac{1}{2\cosh(\pi\chi/2)}\ . \tag{A58}$$

Note that this decays exponentially for large χ, but nevertheless more slowly than does $Q(\eta,\chi)$ for fixed η, from Eq. (A55).

For the *asymmetric case* with $\Upsilon=1$, we have from Eq. (A39) $\psi=2$. The requirement that the distribution of χ be real now fixes k to be purely imaginary. The magnitude of k corresponds to the overall, non-universal, scale-factor; hence we may take $k=\mp i$. We then have

$$\hat{Q}_{\pm}(\eta,\omega)=\frac{\sqrt{\mp i\omega}}{\sinh\sqrt{\mp i\omega}}e^{-\eta\sqrt{\mp i\omega}\coth\sqrt{\mp i\omega}} \tag{A59}$$

(with the same branch of the square root taken in all places). This yields, on integrating over η,

$$Q_{\pm}(\chi)=\frac{1}{2\pi}\int_{-\infty}^{\infty}d\omega\frac{e^{-i\chi\omega}}{\cosh\sqrt{\mp i\omega}}\ . \tag{A60}$$

The solution $\hat{Q}_{+}(\omega)$ with $k=-i$ only has singularities in the lower half plane, and hence $Q_{+}(\chi)$ only has support for *positive* χ. Conversely, Q_{-} only has support for negative χ.

The distribution $Q_{+}(\chi)$ gives, for example, the scaled distribution Eq. (2.31) of the separations, l, between effective nearest-neighbor unpaired spins at scale Γ via $l\approx C\chi\Gamma^2$ with C a nonuniversal coefficient. From Eq. (A60), we see that this distribution falls off exponentially for $l\gg\Gamma^2$, since the nearest singularity to the origin in the complex ω plane is at $\omega=-(i/4)\pi^2$. For small χ, it can be shown (see, e.g., Ref. 11) that

$$Q(\chi)\sim\frac{1}{\chi^{3/2}}e^{-1/(4\chi)} \tag{A61}$$

so that the probability of an effective nearest-neighbor separation of $l \ll \Gamma^2$ at scale Γ is extremely small. From the behavior of Eq. (A59), for the transformed joint distribution, one can show that η and χ are positively correlated, i.e., that long bonds tend to be weaker than short ones, as expected physically.

We now turn to the case of general Υ. In general, Eq. (A50) for $A(\omega)$ cannot be solved in terms of simple functions. Nevertheless, the value of ψ can be found by the condition that $A(\omega)$ be analytic at $\omega=0$ corresponding to the condition that there *not* be a power-law tail for large χ. For the *asymmetric case,* A should have a Taylor expansion in ω starting with ω^1. From the small ω behavior of Eq. (A50), this can only occur if ψ is given by Eq. (A39) yielding $\psi_{\text{asym}}(\Upsilon=1)=2$, as from the exact solution Eq. (A52). For the *symmetric case,* $A(\omega)$ must be even in ω, hence its Taylor series starts with ω^2 yielding Eq. (A43) for $\psi_{\text{sym}}(\Upsilon=1)$.

For the case $\Upsilon=0$, the equation for $A(\omega)$ becomes an ODE which, by the transformation $i\omega=e^{-\tau}$ becomes the equation of motion of a "particle" $A(\tau)$ with damping in an unstable potential $V_{\text{eff}}(A)=-e^{A}+A$. The behavior of the asymmetric solution can then be analyzed in substantial detail, yielding, as for the $\Upsilon=1$ case, exponential decay of $Q(\chi)$ for large χ and $\chi^{-\alpha}e^{-c/\chi}$ behavior for small χ. In the symmetric case, there is again exponential decay for large $|\chi|$. We will not go into the details here, but a related analysis is used to obtain the magnetization of the random transverse field Ising chain discussed elsewhere.[11]

For general $0<\Upsilon<1$, in particular with $\Upsilon=\frac{1}{2}$ as needed in Sec. IV C, the equation for $A(\omega)$ is not a simple ODE. We expect that a similar analysis to the $\Upsilon=0$ case would nevertheless yield the behavior for large and small χ, but we have not carried this out.

6. Random anisotropy

We finally analyze the more complicated situation needed for the *XXZ* chain with random anisotropy. Here we have, for the logarithm of the anisotropy $D\equiv\ln(J^z/J^\perp)$, the recursion relation

$$\tilde{D}=D_1+D_3+\max(D_2,0) \tag{A62}$$

when bond D_2 is decimated. We are interested in fixed points for the scaled variables

$$\theta\equiv D/\Gamma^{\psi} \tag{A63}$$

and $\eta=\zeta/\Gamma$ with ζ obeying the recursion relation Eq. (A3).

It is useful to consider a generalization of Eq. (A61),

$$\tilde{\theta}=\theta_1+\theta_3+\max(\theta_2,M) \tag{A64}$$

with $-\infty\le M\le 0$. For general M, we expect *three* fixed points for the joint distribution $Q(\eta,\theta)$: one with support only for positive θ and exponent ψ_+, which will be manifestly independent of M; one with support only for negative θ with exponent ψ_-, which will depend on M with the $M=0$ and $M=-\infty$ limits simple, and an unstable critical fixed point with support for both positive and negative θ and exponent ψ. For the positive fixed point, we have from the previous analysis, $\psi_+=2$ since $\max(\theta_2,M)=\theta_2$. For the negative fixed point, we have $\psi_-(M=0)=\frac{1}{2}(1+\sqrt{5})$ and $\psi_-(M=-\infty)=2$. For the critical fixed point, the only simple limit is $M=-\infty$; from our earlier analysis we obtain for this case $\psi(M=-\infty)=1$. The critical fixed point will have little weight for large negative θ. Thus, $M=-\infty$ should not be a singular limit and we hypothesize that the critical $\psi(M)$ is *continuous.* We will now show that, for all of the fixed points, the possible range of ψ is restricted.

As for the simpler cases analyzed above, we consider the generating function for the conditional moments

$$\hat{C}(\eta,\omega)\equiv\int_{-\infty}^{\infty}d\theta\, C(\eta,\theta)e^{i\theta\omega}\ , \tag{A65}$$

where

$$C(\eta,\theta)\equiv\text{Prob}(\theta|\eta)=Q(\eta,\theta)/e^{-\eta}\ . \tag{A66}$$

Then $\hat{C}$ satisfies Eq. (A46) with

$$\hat{W}(\omega)=e^{iM\omega}\int_{-\infty}^{M}C(0,\theta)d\theta+\int_{M}^{\infty}C(0,\theta)e^{i\theta\omega}d\theta\ . \tag{A67}$$

A solution of the form Eq. (A47) again exists with $\hat{C}(0,\omega)=e^{A(\omega)}$ yielding $C(0,\theta)$ in terms of A and thereby a complicated relationship between $\hat{W}(\omega)$ and $A(\omega)$. The resulting equation (A47) for $A(\omega)$ cannot be solved explicitly, but useful information can be gleaned by expanding for small ω, i.e., looking at the conditional moments, writing

$$A=i\omega a_1-\tfrac{1}{2}\omega^2a_2+\cdots \tag{A68}$$

and similarly

$$\hat{W}=1+i\omega w_1-\tfrac{1}{2}\omega^2w_2+\cdots\ . \tag{A69}$$

For $\eta=0$, the cumulants of $C(0,\theta)$ are just the Taylor coefficients of A, hence

$$c_{00}=1,\quad c_{01}=a_1,\quad c_{02}=a_2+a_1^2,\quad \text{etc.}\ , \tag{A70}$$

where

$$c_{0p}\equiv\int_{-\infty}^{\infty}\theta^pC(0,\theta)d\theta=C_p(\eta=0)\ . \tag{A71}$$

Similarly, the W_p are moments of the distribution

$$W(\theta)=C(0,\theta)\Theta(\theta-M)+\delta(\theta-M)\int_{-\infty}^{M}C(0,\theta')d\theta' \tag{A72}$$

with Θ the Heaviside step function.

Clearly, there are some necessary inequalities between the moments of $C(0,\theta)$ and those of $W(\theta)$, in particular

$$w_1\ge c_{01}=a_1\ . \tag{A73}$$

The most useful inequalities can be obtained from the moments l_p of a third distribution

$$L(\theta)\equiv\frac{1}{C_<}C(0,\theta)\Theta(M-\theta)\ , \tag{A74}$$

where

$$C_<\equiv\int_{-\infty}^{M}C(0,\theta')d\theta' \tag{A75}$$

is a normalization factor. We have from the definitions of the distributions,

$$w_p=C_<M^p+c_{0p}-C_<l_p\ . \tag{A76}$$

Since L is a probability distribution, we have

$$l_2\geq l_1^2\ , \tag{A77}$$

whence, from Eq. (A76),

$$c_{02}-w_2\geq\frac{(\omega_1-c_{01})^2}{C_<}-2M(w_1-c_{01})\geq(w_1-c_{01})^2 \tag{A78}$$

where the second inequality follows from $C_<\leq 1$, $M\leq 0$, and $w_1\geq c_{01}$. From Eq. (A50), we have

$$w_1=a_1(\psi^2-\psi-1) \tag{A79}$$

and

$$w_2=a_2(4\psi^2-2\psi-1)+a_1^2(1+2\psi-2\psi^2)\ . \tag{A80}$$

From the inequality Eq. (A78) and Eqs. (A70), (A79), and (A80), we then have

$$a_2[4\psi^2-2\psi-2]\leq a_1^2[-(\psi^2-\psi)^2+6(\psi^2-\psi)-4]\ . \tag{A81}$$

But a_2 must be non-negative, since it is the second cumulant of $C(0,\theta)$, hence either the left side of Eq. (A81) must be negative or the right side positive. The first occurs for $\psi\leq 1$, while the second occurs for $3-\sqrt{5}\leq\psi^2-\psi\leq 3+\sqrt{5}$. Therefore, either

$$\psi\leq 1\quad\text{or}\quad 1.507\leq\psi\leq 2.842\ . \tag{A82}$$

The positive and negative solutions lie in the upper range, however, the critical fixed point for $M=-\infty$ has $\psi=1$. Thus, by continuity, we expect that the critical ψ will lie in the lower range of Eq. (A82) for all $M\leq 0$. Note that, in principle, there could be several fixed points with ψ in this range. We are interested in the least unstable of these, the one with only one positive eigenvalue, λ, for perturbations away from it. Numerical solution for $\hat{C}(0,\omega)$ from Eqs. (A46), (A47), and (A67) should be possible and the renormalization-group flows near to this fixed point could be used to calculate λ. Alternatively, a direct numerical study of the recursion relations (A3) and (A62) might also yield both the desired fixed point and λ from a scaling fit.

---

[1]For a recent review, see E. Fradkin, *Field Theories of Condensed Matter Systems* (Addison-Wesley, Redwood City, CA, 1991).

[2]C. A. Doty and D. S. Fisher, Phys. Rev. B **45**, 2167 (1992).

[3]T. P. Eggarter and R. Riedinger, Phys. Rev. **18**, 569 (1978), and references therein.

[4]A. Klein and J. F. Perez, Commun. Math. Phys. **128**, 99 (1990).

[5]R. Shankar and G. Murthy, Phys. Rev. B **36**, 536 (1987); **35**, 3671 (1987).

[6]B. M. McCoy and T. T. Wu, Phys. Rev. **176**, 631 (1968); **188**, 982 (1969); B. McCoy, *ibid.* **188**, 1014 (1969).

[7]S. White and D. A. Huse, Phys. Rev. B **48**, 3844 (1993).

[8]C. Dasgupta and S. K. Ma, Phys. Rev. B **22**, 1305 (1980).

[9]S. K. Ma, C. Dasgupta, and C.-K. Hu, Phys. Rev. Lett. **43**, 1434 (1979).

[10]R. N. Bhatt and P. A. Lee, Phys. Rev. Lett. **48**, 344 (1982).

[11]D. S. Fisher, Phys. Rev. Lett. **69**, 534 (1992); and (unpublished).

[12]R. J. Baxter, Ann. Phys. (N.Y.) **70**, 193 (1972).

[13]See, e.g., M. C. Cross and D. S. Fisher, Phys. Rev. B **19**, 402 (1979), and references therein.

[14]Note, however, that near the ferromagnetic end of the *XX* fixed line of the pure system, the irrelevance of weak randomness certainly implies breakdown of the present RG procedure. Warning of this is provided by the approximate recursion relations Eq. (2.3): in this limit, some of the new effective $\tilde{J}$'s will be *larger* than those decimated, invalidating the RG procedure.

[15]It may be possible to calculate some of the corrections for the *XX* case by the methods of Ref. 11.

[16]McCoy (Ref. 6) has computed the distribution of boundary spontaneous magnetization for the semi-infinite random transverse field Ising chain. In Ref. 11, both this and the mean boundary magnetization are computed by the present methods. The extreme difference between average and typical is seen explicitly.

[17]In Ref. 4 it is proved that for an *XX* chain in a random *Z* field, the correlation function decays exponentially with probability one.

[18]If the chains have fourfold symmetry in the pure system, then randomness in a chain will not induce exchange anisotropy. However, distortions, etc., due to randomness in *other* chains could introduce weak random, statistically isotropic *XY* anisotropy.

[19]F. D. M. Haldane, Phys. Rev. Lett. **50**, 1153 (1983); Phys. Lett. **93A**, 464 (1983).

[20]M. A. Paadenen, S. Sachdev, R. N. Bhatt, and A. E. Ruckenstein, Phys. Rev. Lett. **57**, 2061 (1986); M. A. Paalenen, J. E. Graebner, R. N. Bhatt, and S. Sachdev, *ibid.* **61**, 597 (1988).

[21]R. N. Bhatt and D. S. Fisher, Phys. Rev. Lett. **68**, 3072 (1992).

[22]M. P. A. Fisher, P. B. Weichman, G. Grinstein, and D. S. Fisher, Phys. Rev. B **40**, 546 (1989).